Histological examination showed that *Nppc* mice had wider growth plates than their nontransgenic littermates (Fig. 1d). In the tibiae of 2-week-old mice, the proliferative and hypertrophic chondrocyte layers express type II and X collagens, respectively, as shown by *in situ* hybridization (see Supplementary Fig. 2 online). These layers were significantly wider in *Nppc* mice than in nontransgenic mice (proliferative: 234 ± 12 versus 207 ± 14 μm, $P < 0.05$; hypertrophic: 215 ± 3 versus 193 ± 16 μm, $P < 0.05$). The intensities of *Col2a1* and *Col10a1* mRNA expression did not differ between the two genotypes. Each hypertrophic chondrocyte was enlarged in *Nppc* mice as compared with their nontransgenic littermates (Fig. 1d and Supplementary Fig. 2 online). Von Kossa staining of the proximal tibiae showed that subchondral trabeculae were more abundant and longer in *Nppc* mice than in nontransgenic mice (Fig. 1e). In addition, assessment by peripheral quantitative computed tomography (pQCT) showed that the bone mineral density of trabecular bones in the proximal tibiae of 12-week-old *Nppc* mice is significantly larger than that of their nontransgenic littermates (202.2 ± 6.4 versus 188.3 ± 5.3 g/mm^3, $P < 0.05$).

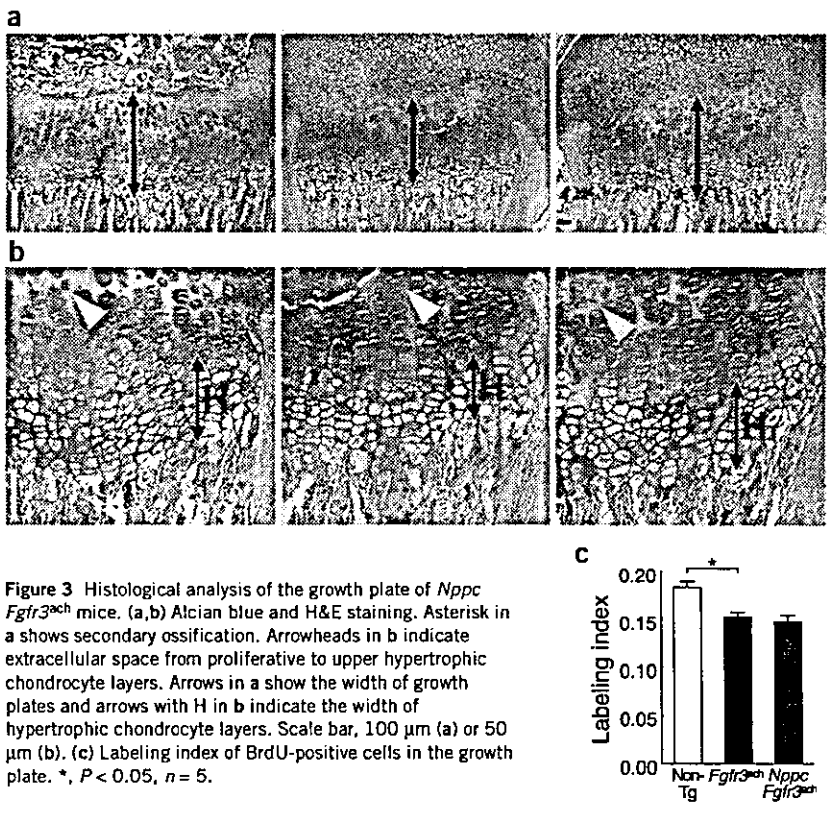

Figure 3 Histological analysis of the growth plate of *Nppc Fgfr3*^{ach} mice. (a,b) Alcian blue and H&E staining. Asterisk in a shows secondary ossification. Arrowheads in b indicate extracellular space from proliferative to upper hypertrophic chondrocyte layers. Arrows in a show the width of growth plates and arrows with H in b indicate the width of hypertrophic chondrocyte layers. Scale bar, 100 μm (a) or 50 μm (b). (c) Labeling index of BrdU-positive cells in the growth plate. *, $P < 0.05$, $n = 5$.

Gross phenotypes of *Nppc Fgfr3*^{ach} mice

To study the effects of CNP on dwarfism in *Fgfr3*^{ach} mice, we created *Fgfr3*^{ach} mice with targeted overexpression of CNP in cartilage by cross-mating *Fgfr3*^{ach} mice with *Nppc* mice. We confirmed the expression of the *Col2a1-Nppc* transgene in the cartilage of the resultant double transgenic (*Nppc Fgfr3*^{ach}) mice (data not shown). We also confirmed, by quantitative RT-PCR analysis, that the amount of *Fgfr3*^{ach} expression in the cartilage of *Nppc Fgfr3*^{ach} mice is no different from that in the cartilage of *Fgfr3*^{ach} mice, indicating that overexpression of CNP does not alter the expression of the *Fgfr3*^{ach} transgene (Fig. 2a).

The growth curve and soft x-ray analysis of *Nppc Fgfr3*^{ach} mice showed that the shortening of *Fgfr3*^{ach} mice is rescued by overexpression of CNP in the growth-plate cartilage (Fig. 2b,c). At the age of 10 weeks, the naso-anal length of *Nppc Fgfr3*^{ach} mice was 94.7 ± 4.0 mm, 8% larger than that of *Fgfr3*^{ach} mice (87.7 ± 2.6 mm) and comparable to that of their nontransgenic littermates (97.0 ± 4.2 mm) (Fig. 2b). The shortening of bones formed through endochondral ossification in 3-month-old female *Fgfr3*^{ach} mice, measured on the soft x-ray film, was rescued in *Nppc Fgfr3*^{ach} mice (Fig. 2d). The width of the cranium did not differ among the three genotypes (Fig. 2d).

To investigate the dose-response effect of CNP on the growth of achondroplastic bones, we generated *Fgfr3*^{ach} mice homozygous for the *Col2a1-Nppc* transgene. The relative abundance of CNP protein in the cartilage of neonatal mice, as estimated by immunohistochemical staining, was *Nppc*-homozygous *Fgfr3*^{ach} > *Nppc*-heterozygous *Fgfr3*^{ach} > *Fgfr3*^{ach} (Fig. 2e). The immunostaining intensities measured using NIH Image software[23] were 145% and 127% as high in the cartilage of *Nppc*-homozygous *Fgfr3*^{ach} and *Nppc*-heterozygous *Fgfr3*^{ach} mice, respectively, as in that of *Fgfr3*^{ach} mice. The dwarfing bones of *Fgfr3*^{ach} mice were elongated dose-dependently in *Nppc*-homozygous *Fgfr3*^{ach} and *Nppc*-heterozygous *Fgfr3*^{ach} mice (Fig. 2f).

Histological analysis of *Nppc Fgfr3*^{ach} mice

Microscopic analysis of tibial growth plates from 2-week-old mice showed that the decreased width of the growth plate of *Fgfr3*^{ach} mice (169 ± 15 μm) is rescued in *Nppc Fgfr3*^{ach} mice (229 ± 21 μm) and is comparable to that of their nontransgenic littermates (220 ± 15 μm) (Fig. 3a). Higher magnification showed that the decreased extracellular space between the proliferative and the upper hypertrophic chondrocyte layers of *Fgfr3*^{ach} mice was restored in *Nppc Fgfr3*^{ach} mice and could be as large as in nontransgenic littermates (Fig. 3b). *In situ* hybridization analysis showed that the width of the hypertrophic chondrocyte layer expressing *Col10a1* mRNA was also restored in *Nppc Fgfr3*^{ach} mice, although there was no appreciable difference in expression intensity between genotypes (see Supplementary Fig. 3 online). There was also no difference in the intensity of *Col2a1* mRNA expression (data not shown). In the proximal tibia of 2-week-old mice, the secondary ossification center was well organized in nontransgenic mice, whereas it was not yet formed in either their *Fgfr3*^{ach} or *Nppc Fgfr3*^{ach} littermates, indicating that overexpression of CNP does not affect the delayed differentiation of chondrocytes in achondroplastic growth plates (Fig. 3a). The secondary ossification centers in the tibiae of both *Fgfr3*^{ach} and *Nppc Fgfr3*^{ach} mice were formed about 3 d later than in nontransgenic tibia. The number of bromodeoxyuridine (BrdU)-positive chondrocytes was significantly lower in the growth plates of *Fgfr3*^{ach} mice, as previously reported[19], whereas there was no difference in the number of BrdU-positive chondrocytes in the growth plates of *Fgfr3*^{ach} and *Nppc Fgfr3*^{ach} mice (Fig. 3c and Supplementary Fig. 4 online). This indicates that overexpression of CNP does not change the decreased proliferation of chondrocytes in *Fgfr3*^{ach} mice.

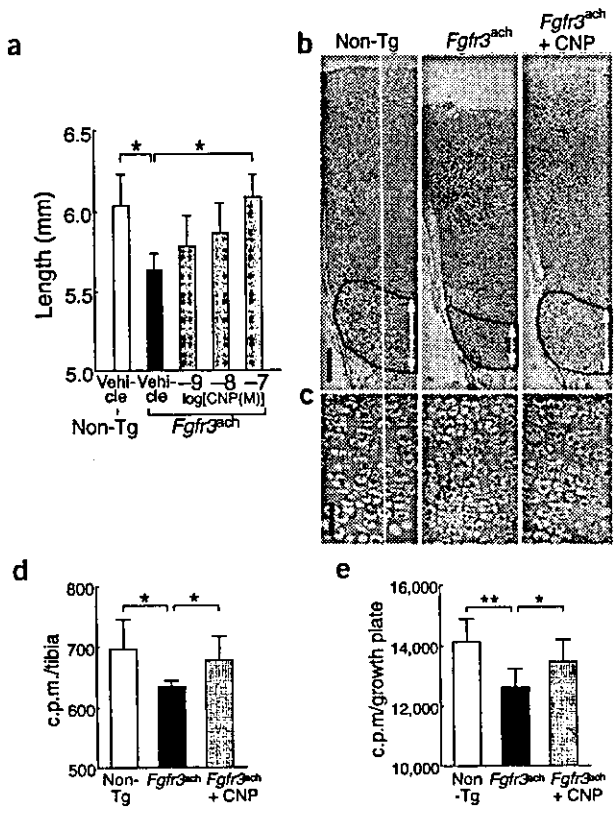

Figure 4 Effects of CNP on cultured tibiae from *Fgfr3*^{ach} mice. (a) Tibial lengths at the end of culture period. *, $P < 0.05$, $n = 5$–6. (b) Histological pictures of tibiae of nontransgenic mice, tibiae of *Fgfr3*^{ach} mice and CNP-treated tibiae of *Fgfr3*^{ach} mice. Arrows indicate the width of hypertrophic chondrocyte layers demarcated in the figures. (c) Highlight of the prehypertrophic chondrocyte layers from b. Scale bar, 200 μm (b) or 50 μm (c).(d,e) [^{35}S]sulfate (d) and [^{3}H]proline (e) incorporation into cartilage into tibiae of nontransgenic mice, *Fgfr3*^{ach} mice and *Fgfr3*^{ach} mice with CNP treatment. * and **, $P < 0.05$ and $P < 0.01$, respectively, $n = 5$–6 (d) and 9 (e).

Effects of CNP on cultured tibiae from *Fgfr3*^{ach} mice

To confirm the direct effect of CNP on bone growth in *Fgfr3*^{ach} mice, we carried out organ culture experiments using tibiae from fetal *Fgfr3*^{ach} mice. The fetal tibiae of *Fgfr3*^{ach} mice at 16.5 days post coitus (dpc) were shorter than those of their nontransgenic littermates (data not shown). CNP (10^{-9}–10^{-7} M) caused elongation of explanted tibiae from fetal *Fgfr3*^{ach} mice in a dose-dependent manner; those treated with 10^{-7} M CNP reached lengths as great as those of vehicle-treated tibiae from nontransgenic mice by the end of the culture period (Fig. 4a). Microscopic analysis showed that the width of the hypertrophic chondrocyte layer in cultured tibiae from *Fgfr3*^{ach} mice, which is lower than that in tibiae of nontransgenic mice, was restored by treatment with 10^{-7} M CNP (Fig. 4b). With higher magnification, we observed that the decreased extracellular space between the proliferative and the prehypertrophic chondrocyte layers of the tibiae of *Fgfr3*^{ach} mice was normalized by 10^{-7} M CNP (Fig. 4c). In fact, although the basal synthesis of glycosaminoglycan, measured by [^{35}S]sulfate incorporation, was much lower in tibiae from *Fgfr3*^{ach} mice than in those from nontransgenic mice, 10^{-7} M CNP increased glycosaminoglycan synthesis in tibiae from *Fgfr3*^{ach} mice to a level as high as in vehicle-treated tibiae from nontransgenic mice (Fig. 4d). The same dose of CNP also increased the synthesis of cartilage collagen, as estimated from the uptake of [^{3}H]proline into growth plates from *Fgfr3*^{ach} mice, to a level comparable to that in the growth plates from nontransgenic mice (Fig. 4e).

Effects of CNP on signaling pathways of FGF

We next investigated the effects of CNP on FGF signaling pathways in growth-plate chondrocytes using cultured tibiae from fetal mice. The treatment of tibial explants with CNP (10^{-6} and 10^{-7} M) or its second messenger, cGMP (10^{-5} M), before addition of FGF-2 (2 ng/ml) markedly decreased the FGF-2-induced phosphorylation of ERK1/2 in a dose-dependent fashion without decreasing the amount of ERK protein (Fig. 5a). In contrast, the same doses of either CNP or cGMP did not alter the FGF-2-induced phosphorylation of STAT-1 (Fig. 5b). Essentially identical results were obtained using the chondrogenic cell line ATDC5 (ref. 24) (data not shown). To further elucidate the effect of CNP on phosphorylation of ERK1/2 *in vivo*, we examined the amounts of phosphorylated ERK1/2 in the cartilage of nontransgenic, *Fgfr3*^{ach}, *Nppc* and *Nppc Fgfr3*^{ach} mice. The abundance of phosphorylated ERK1/2 was greater in the cartilage of *Fgfr3*^{ach} mice, and smaller in the cartilage of *Nppc* mice, than in the cartilage of nontransgenic mice. *Nppc Fgfr3*^{ach} mice, in which the shortening of achondroplastic bones was rescued, showed substantially less elevation of ERK1/2 phosphorylation than was seen in the cartilage of *Fgfr3*^{ach} mice (Fig. 5c). PD98059, an inhibitor of the MAPK cascade[25], increased the total length and width of the growth-plate cartilage of tibiae from both fetal *Fgfr3*^{ach} and nontransgenic mice in organ culture (Fig. 5d). PD98059 increased the length of tibiae from *Fgfr3*^{ach} mice more than that of tibiae from nontransgenic mice, in parallel with the level of cartilage matrix synthesis estimated from [^{35}S]sulfate and [^{3}H]proline incorporation (Fig. 5e–g). There was no difference in the proliferation of chondrocytes in tibiae, measured by BrdU uptake, between PD98059- and vehicle-treated groups of either genotype (labeling indexes: nontransgenic, 0.252 ± 0.029 versus 0.248 ± 0.025, respectively; *Fgfr3*^{ach}, 0.221 ± 0.025 versus 0.225 ± 0.027, respectively). We obtained the same results using U0126, another MEK inhibitor (data not shown).

DISCUSSION

This study demonstrates that targeted overexpression of CNP in cartilage counteracts dwarfism in *Fgfr3*^{ach} mice, a model of human achondroplasia. We previously showed, using transgenic and knockout mice, that the CNP–GC-B system is important in endochondral ossification[11–13]. The *Nppc* mice developed in this study showed skeletal overgrowth with widened growth plates, a phenotype resembling that of FGFR-3-depleted mice[17,18] and opposite to those of *Fgfr3*^{ach} mice[19] and *Nppc* knockout mice[13]. This indicates that the CNP–GC-B system may counteract the FGFs–FGFR-3 system in endochondral ossification. Here, we show that activation of the CNP–GC-B system reverses the FGFR-3-mediated inhibition of the endochondral ossification in achondroplasia. Activation of the CNP–GC-B system in chondrocytes of the growth plate therefore represents a potential new therapeutic strategy for human achondroplasia caused by a constitutively active mutation in *FGFR3*.

Constitutive activation of FGFR-3 has been reported to inhibit the growth of long bones made through endochondral ossification by decreasing the proliferation and delaying the differentiation of

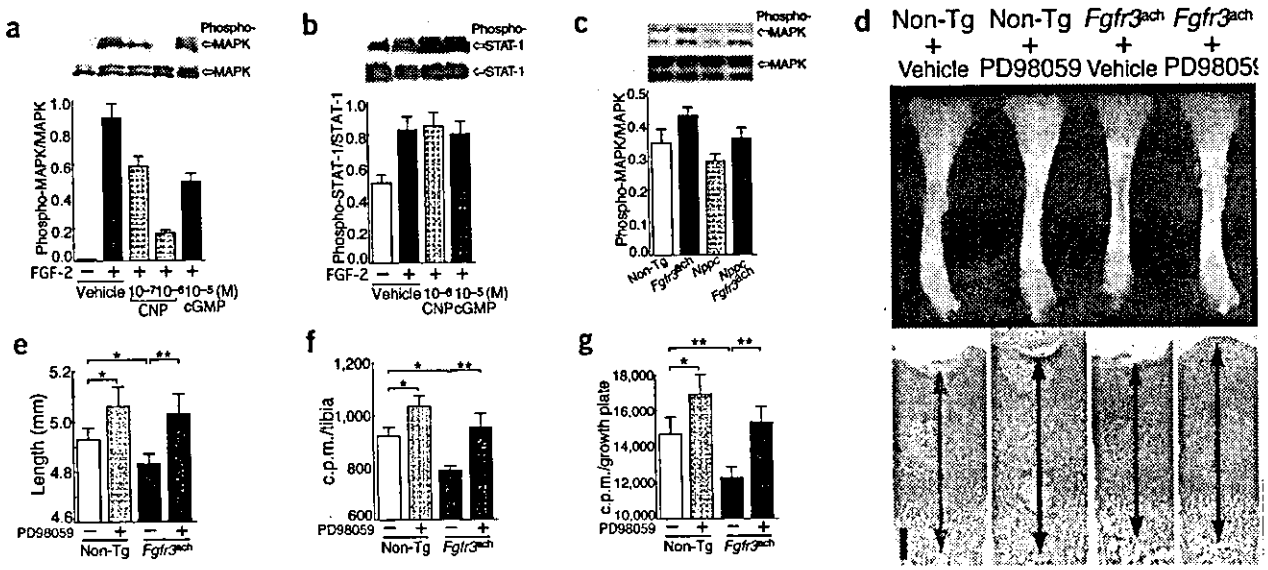

Figure 5 Intracellular signaling analysis. (a–c) Western blotting for phosphorylated MAPK (a) and STAT-1 (b) in explanted tibiae, and phosphorylated MAPK in growth-plate cartilage from neonatal mice (c). (d–g) Effects of PD98059 on cultured *Fgfr3*^{ach} tibiae. Gross appearance (upper) and histological picture of the growth plate (d), tibial length (e), [^{35}S]sulfate incorporation (f) and [^{3}H]proline uptake (g) in each group. Arrows in d indicate the width of the growth-plate cartilage. * and ** in e–g, $P < 0.05$ and $P < 0.01$, respectively, $n = 4$–5. Scale bar, 200 μm (d).

growth-plate chondrocytes via the STAT-1 pathway[6,19]. In the present study, however, we determined that CNP does not affect the amount of phosphorylated STAT-1 induced by FGF-2 either in explanted tibiae or in the chondrogenic cell line ATDC5. In addition, we showed that overexpressed CNP does not restore either the decreased BrdU uptake or the delayed formation of secondary ossification centers in the growth-plate cartilage of *Fgfr3*^{ach} mice (Fig. 3). Thus, CNP does not correct either the decreased proliferation or the delayed differentiation of achondroplastic growth-plate chondrocytes *in vivo*. These results show that CNP does not correct the STAT-1-mediated bone growth inhibition of activated FGFR-3. On the other hand, we show that constitutive activation of FGFR-3 inhibits longitudinal bone growth by decreasing the extracellular matrix synthesis through the MAPK pathway, indicating that MEK inhibitors (i) increase the extracellular matrix synthesis of explanted tibiae, as estimated by incorporation of [^{35}S]sulfate and [^{3}H]proline, more strongly in tibiae of *Fgfr3*^{ach} mice than in those of nontransgenic mice; (ii) do not alter the proliferation of chondrocytes, as estimated by BrdU uptake, in the tibiae of both *Fgfr3*^{ach} and nontransgenic mice; and (iii) elongate cultured tibiae from *Fgfr3*^{ach} mice more strongly than those from nontransgenic mice (Fig. 5e–g). In addition, we show that CNP markedly decreases the FGF-2-induced phosphorylation of ERK1/2 both in explanted tibiae and in ATDC5 cells, confirming that CNP interferes with activation of the MAPK pathway downstream of FGFR-3 signaling in the growth-plate cartilage, as we and other groups have previously reported in mesangeal cells[21] and fibroblasts[20]. We have further confirmed this finding using *in vivo* animal models, including *Nppc Fgfr3*^{ach} mice. Accordingly, we conclude that the mechanism by which CNP counteracts the dwarfism of achondroplastic bones in *Fgfr3*^{ach} mice is by restoring the MAPK-mediated inhibition of extracellular matrix production in the growth-plate cartilage of achondroplastic bones (Fig. 6). The role of the MAPK pathway in FGF signaling in chondrocytes has not been extensively studied so far, and the results of previous studies using cell culture were complicated and contradictory[26,27]. In the present study, we used both *ex vivo* organ culture and cell culture to elucidate the role of the MAPK pathway in endochondral bone elongation directly and in detail, and the two sets of results corresponded well. De Crombrugghe *et al.* have recently reported that constitutive activation of MEK1 in chondrocytes induces dwarfism that resembles achondroplasia (S. Murakami, S. McKinney, D. Givol, and B. de Crombrugghe, personal communication). These results support our hypothesis that the CNP–GC-B system rescues achondroplastic dwarfism by inhibiting the MAPK pathway of FGFR-3 signaling in the regulation of bone growth.

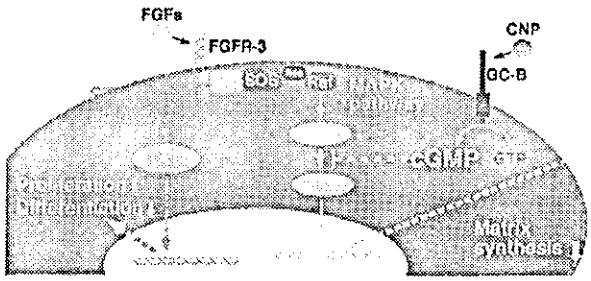

Figure 6 Schematic representation of the mechanism by which CNP compensates for FGFR-3-mediated shortening of bones. FGFR-3 inhibits endochondral bone growth by inhibiting proliferation and differentiation of growth-plate chondrocytes through the STAT-1 pathway and by decreasing extracellular matrix synthesis through the MAPK pathway. cGMP, the second messenger of CNP–GC-B, inhibits the MAPK pathway of FGFR-3 signaling, restores the decreased synthesis of the extracellular matrix and partially counteracts the dwarfism of achondroplastic bones.

Bone morphogenetic protein-2 (BMP-2) and BMP-4 have recently been reported to counteract the growth-inhibitory effect of FGFR-3 on explanted bones from the same achondroplastic model mice by restoring the proliferation of achondroplastic growth-plate chondrocytes[28]. Although the nature of intracellular interactions between FGF and BMP signaling in chondrocytes remains unclear, CNP and BMP might complementarily reverse the inhibitory effect of FGF on bone growth suggesting the possibility of a new combined therapy for achondroplasia.

Current therapies for achondroplasia include distraction osteogenesis[29,30], an orthopedic procedure, and administration of growth hormone[31]. Although distraction osteogenesis gives better results, it limits the quality of a patient's life. Growth hormone has only minimal effect on achondroplasia, has been reported to aggravate body disproportion in some case[32] and is very costly. According to our unpublished results, the maximal growth-promoting effect of CNP (10^{-7} M) on cultured fetal bones is much stronger than that of growth hormone (100 ng/ml), IGF-I (100 ng/ml)[33] or other skeletal growth regulators, including BMP-2 (100 ng/ml), BMP-4 (100 ng/ml), TGF-β_2 (100 ng/ml)[34] and PTH (100 ng/ml)[35], under identical experimental conditions. Activation of the CNP–GC-B system in chondrocytes may thus be a prospective means to treat achondroplasia. Activation of GC-B resulting from elevated plasma concentrations of BNP[11] or CNP (unpublished data) in transgenic mice using a promoter of serum amyloid P component causes skeletal overgrowth. This indicates that specific activators of the CNP–GC-B system could be delivered via the general circulation as therapy for achondroplasia. Considering the minimal hypotensive effect of CNP compared with the other natriuretic peptides ANP and BNP, systemic administration of CNP could be of practical use as a means to activate the CNP–GC-B system in the growth-plate chondrocytes. In addition, overexpression of CNP in cartilage increased bone mineral density, as estimated by pQCT, in the trabecular bone adjacent to the growth-plate cartilage, suggesting that the activation of the CNP–GC-B system in endochondral cartilage template formation positively affects the properties of bone produced from this template. This effect could be beneficial to patients with achondroplasia treated with CNP.

We observed a gender difference in the promoting effect of CNP on bone growth in the present study, but the reasons for this observation are unclear at present. Further studies are ongoing in our laboratory.

In conclusion, the present study demonstrates a potential new therapeutic strategy for human achondroplasia involving activation of the CNP–GC-B system in the chondrocytes of the growth plate.

METHODS

Generation and identification of *Nppc* mice. A 489-base-pair mouse *Nppc* cDNA[36] was inserted into a 6.5-kilobase segment of the *Col2a1* promoter region[22], at a site within the first intron. The assembled transgene (*Col2a1-Nppc*) was microinjected into fertilized C57BL/6 oocytes and the resultant transgenic mice were identified by Southern blotting. *Sac* I digestion of mouse genomic DNA containing *Col2a1-Nppc* yielded additional hybridizing DNA species of ~2.1 kilobases, whereas the intrinsic *Nppc* gene was recognized as DNA species of ~3.0 kilobases[37]. We assessed the transgene copy number on the basis of the density of the band compared with that of the intrinsic *Nppc* band as determined using densitometry.

Generation of the doubly transgenic mice of *Col2a1-Nppc* and *Fgfr3*^{ach}. Generation of transgenic mice that express an activated FGFR-3 in the growth plate (*Fgfr3*^{ach} mice) using *Col2a1* promoter and enhancer sequences was reported previously[19]. In all experiments using this achondroplastic model, we used transgenic mice carrying the heterozygous *Fgfr3*^{ach} transgene. To generate doubly transgenic mice for *Col2a1-Nppc* and *Fgfr3*^{ach}, *Nppc* mice were mated with *Fgfr3*^{ach} mice. The resultant *Nppc Fgfr3*^{ach} mice and *Nppc* mice were then mated to generate *Fgfr3*^{ach} mice homozygous for *Col2a1-Nppc*. All of the experimental procedures were approved by the Kyoto University Graduate School of Medicine committee on animal research.

Detection of mRNA expression of transgenes. To detect expression of *Col2a1-Nppc*, we carried out RT-PCR using as the forward primer a sequence located in the exon I of the *Col 2a1* gene and as the reverse primer a sequence from *Nppc* cDNA. The resultant PCR product of 450 base pairs was then recognizable as a transcript of the transgene from which the ~3-kilobase intron I of *Col2a1* had been spliced out. Expression of the *Fgfr3*^{ach} transgene was estimated by a quantitative RT-PCR method based on kinetic analysis[38,39], using primers for *Fgfr3*^{ach} and *Gapd*, as previously reported[19,39].

Skeletal morphology and pQCT analysis. For visualization of the whole skeleton, cleared skeletons of newborn mice were stained with Alizarin red S and Alcian blue[11]. To observe skeletons in adulthood, 3-month-old female mice were subjected to soft x-ray analysis[11], and the lengths of bones were measured on the soft x-ray film. To evaluate the bone mineral density of trabecular bones in the proximal tibiae, tibiae were subjected to pQCT analysis, using an XCT Research SA instrument (Stratec Medizintechnik), as previously reported[40].

Histological analysis. For light microscopy, sections were cut from paraffin-embedded specimens and stained with Alcian blue and hematoxylin-eosin (H&E). For BrdU staining, 2-week-old mice were injected intraperitoneally with BrdU (100 μg per gram body weight) and were killed 1 h later[19]. The labeling index in the proliferative chondrocyte layer was analyzed using National Institutes of Health (NIH) freeware. To evaluate the mineralized stage, von Kossa staining was done on undecalcified sections[13]. Immunohistochemical staining for CNP was carried out on frozen sections of neonatal mouse ribs using the ImmunoStaining Detection Kit (Peninsula). Intensity of immunostaining was analyzed using NIH freeware as previously described[23]. *In situ* hybridization analysis was carried out on 2-week-old mice tibiae using digoxigenin-labeled antisense and sense riboprobes obtained from rat *Col2a1* and *Col10a1* cDNA fragments[41].

Organ culture. Tibiae from *Fgfr3*^{ach} fetuses or their nontransgenic littermates were dissected out at 16.5 dpc and cultured for 4 d by the suspension culture technique[12] with the indicated doses of CNP or with biochemical inhibitors of MEK, PD98059 (50 μM, Cell Signaling) or U0126 (10 μM, Promega). Glycosaminoglycan synthesis in the cultured tibiae was assessed by measuring [^{35}S]sulfate incorporation as previously described[42], using 5 μCi/ml [^{35}S]sulfate in the medium. The synthesis of cartilage collagen was assessed by measuring uptake of [^{3}H]proline (20 μCi/ml in the medium) into cartilage collagen isolated from papain digests of the proximal tibial growth-plate cartilage[43]. The proliferation of chondrocytes in explanted tibiae was assessed by measuring BrdU incorporation as described before[12]. cGMP production was measured by radioimmunoassay[44] using cultured tibiae from *Nppc* or nontransgenic fetuses of 16.5 dpc at the end of the 4-d culture period.

Intracellular signaling analysis. Tibial explants from fetal mice of 16.5 dpc were incubated with 10^{-7}–10^{-6} M CNP or 10^{-5} M cGMP for 1 h, and then FGF-2 (2 ng/ml) was added for 5 min. ATDC5 cells on day 11 after confluency were incubated with the same doses of CNP or cGMP for 1 h, and then FGF-2 (1 ng/ml) was added for 3 min. Explanted tibiae, ATDC5 cells and tibial growth plates freshly dissected out from neonatal nontransgenic, *Fgfr3*^{ach}, *Nppc* and *Nppc Fgfr3*^{ach} mice were homogenized and lysed, and then western blotting was carried out using antibodies to phosphorylated ERK1/2 (Promega), ERK1/2 (BD Bioscience), phosphorylated STAT-1 (Cell Signaling) or STAT-1 (Santa Cruz Biotechnology).

Statistics. Data were expressed as mean ± s.d. and the statistical significance of differences in mean values was assessed by Student's *t*-test or analysis of variance (ANOVA) with Fisher's protected least-significant-difference test, as appropriate. Differences among means were considered significant at values of $P < 0.01$ or $P < 0.05$.

Note: Supplementary information is available on the Nature Medicine website.

ACKNOWLEDGMENTS

We thank D.M. Ornitz (Department of Molecular Biology and Pharmacology, Washington University School of Medicine) for *Fgfr3*^{ach} mice and B. DeCrombrugghe (Department of Molecular Genetics, University of Texas M.D. Anderson Cancer Center) for the *Col2a1* promoter. This work was supported by grants from Research for the Future of the Japan Society for the Promotion of Science (JSPS-RFTF 96100204 and 98L00801); the Japanese Ministry of Education, Sciences, Sports, and Culture (# 12770627); Smoking Research Foundation; Toyobo Biochemical Foundation; and Uehara Memorial Foundation.

COMPETING INTERESTS STATEMENT

The authors declare that they have no competing financial interests.

Received 29 September; accepted 26 November 2003
Published online at http://www.nature.com/naturemedicine/

1. Oberklaid, F., Danks, D.M., Jensen, F., Stace, L. & Rosshandler, S. Achondroplasia and hypochondroplasia. Comments on frequency, mutation rate, and radiological features in skull and spine. *J. Med. Genet.* **16**, 140–146 (1979).
2. Bellus, G.A. *et al.* Achondroplasia is defined by recurrent G380R mutations of FGFR3. *Am. J. Hum. Genet.* **56**, 368–373 (1995).
3. Shiang, R. *et al.* Mutations in the transmembrane domain of FGFR3 cause the most common genetic form of dwarfism, achondroplasia. *Cell* **78**, 335–342 (1994).
4. Cohen, M.M. Jr. Short-limb skeletal dysplasias and craniosynostosis: what do they have in common? *Pediatr. Radiol.* **27**, 442–446 (1997).
5. Boilly, B., Vercoutter-Edouart, A.S., Hondermarck, H., Nurcombe, V. & Le Bourhis, X. FGF signals for cell proliferation and migration through different pathways. *Cytokine Growth Factor Rev.* **11**, 295–302 (2000).
6. Sahni, M. *et al.* FGF signaling inhibits chondrocyte proliferation and regulates bone development through the STAT-1 pathway. *Genes Dev.* **13**, 1361–1366 (1999).
7. Sahni, M., Raz, R., Coffin, J.D., Levy, D. & Basilico, C. STAT1 mediates the increased apoptosis and reduced chondrocyte proliferation in mice overexpressing FGF2. *Development* **128**, 2119–2129 (2001).
8. Nakao, K., Ogawa, Y., Suga, S. & Imura, H. Molecular biology and biochemistry of the natriuretic peptide system. I: Natriuretic peptides. *J. Hypertens.* **10**, 907–912 (1992).
9. Nakao, K., Ogawa, Y., Suga, S. & Imura, H. Molecular biology and biochemistry of the natriuretic peptide system. II: Natriuretic peptide receptors. *J. Hypertens.* **10**, 1111–1114 (1992).
10. Garbers, D.L. Guanylate cyclase receptor family. *Recent. Prog. Horm. Res.* **46**, 85–96 (1990).
11. Suda, M. *et al.* Skeletal overgrowth in transgenic mice that overexpress brain natriuretic peptide. *Proc. Natl. Acad. Sci. USA* **95**, 2337–2342 (1998).
12. Yasoda, A. *et al.* Natriuretic peptide regulation of endochondral ossification. Evidence for possible roles of the C-type natriuretic peptide/guanylyl cyclase-B pathway. *J. Biol. Chem.* **273**, 11695–11700 (1998).
13. Chusho, H. *et al.* Dwarfism and early death in mice lacking C-type natriuretic peptide. *Proc. Natl. Acad. Sci. USA* **98**, 4016–4021 (2001).
14. Pfeifer, A. *et al.* Intestinal secretory defects and dwarfism in mice lacking cGMP-dependent protein kinase II. *Science* **274**, 2082–2086 (1996).
15. Matsukawa, N. *et al.* The natriuretic peptide clearance receptor locally modulates the physiological effects of the natriuretic peptide system. *Proc. Natl. Acad. Sci. USA* **96**, 7403–7408 (1999).
16. Jaubert, J. *et al.* Three new allelic mouse mutations that cause skeletal overgrowth involve the natriuretic peptide receptor C gene (Npr3). *Proc. Natl. Acad. Sci. USA* **96**, 10278–10283 (1999).
17. Colvin, J.S., Bohne, B.A., Harding, G.W., McEwen, D.G. & Ornitz, D.M. Skeletal overgrowth and deafness in mice lacking fibroblast growth factor receptor 3. *Nat. Genet.* **12**, 390–397 (1996).
18. Deng, C., Wynshaw-Boris, A., Zhou, F., Kuo, A. & Leder, P. Fibroblast growth factor receptor 3 is a negative regulator of bone growth. *Cell* **84**, 911–921 (1996).
19. Naski, M.C., Colvin, J.S., Coffin, J.D. & Ornitz, D.M. Repression of hedgehog signaling and BMP4 expression in growth plate cartilage by fibroblast growth factor receptor 3. *Development* **125**, 4977–4988 (1998).
20. Chrisman, T.D. & Garbers, D.L. Reciprocal antagonism coordinates C-type natriuretic peptide and mitogen-signaling pathways in fibroblasts. *J. Biol. Chem.* **274**, 4293–4299 (1999).
21. Suganami, T. *et al.* Overexpression of brain natriuretic peptide in mice ameliorates immune-mediated renal injury. *J. Am. Soc. Nephrol.* **12**, 2652–2663 (2001).
22. Metsaranta, M. *et al.* Developmental expression of a type II collagen/β-galactosidase fusion gene in transgenic mice. *Dev. Dyn.* **204**, 202–210 (1995).
23. Toyokuni, S. *et al.* Quantitative immunohistochemical determination of 8-hydroxy-2'-deoxyguanosine by a monoclonal antibody N45.1: its application to ferric nitrilotriacetate-induced renal carcinogenesis model. *Lab. Invest.* **76**, 365–374 (1997).
24. Shukunami, C. *et al.* Chondrogenic differentiation of clonal mouse embryonic cell line ATDC5 *in vitro*: differentiation-dependent gene expression of parathyroid hormone (PTH)/PTH-related peptide receptor. *J. Cell. Biol.* **133**, 457–468 (1996).
25. Dudley, D.T., Pang, L., Decker, S.J., Bridges, A.J. & Saltiel, A.R. A synthetic inhibitor of the mitogen-activated protein kinase cascade. *Proc. Natl. Acad. Sci. USA* **92**, 7686–7689 (1995).
26. Murakami, S., Kan, M., McKeehan, W.L. & de Crombrugghe, B. Up-regulation of the chondrogenic Sox9 gene by fibroblast growth factors is mediated by the mitogen-activated protein kinase pathway. *Proc. Natl. Acad. Sci. USA* **97**, 1113–1118 (2000).
27. Yoon, Y.M. *et al.* Maintenance of differentiated phenotype of articular chondrocytes by protein kinase C and extracellular signal-regulated protein kinase. *J. Biol. Chem.* **277**, 8412–8420 (2002).
28. Minina, E., Kreschel, C., Naski, M.C., Ornitz, D.M. & Vortkamp, A. Interaction of FGF, Ihh/Pthlh, and BMP signaling integrates chondrocyte proliferation and hypertrophic differentiation. *Dev. Cell* **3**, 439–449 (2002).
29. Noonan, K.J., Leyes, M., Forriol, F. & Canadell, J. Distraction osteogenesis of the lower extremity with use of monolateral external fixation. A study of two hundred and sixty-one femora and tibiae. *J. Bone. Joint. Surg. Am.* **80**, 793–806 (1998).
30. Aldegheri, R. Distraction osteogenesis for lengthening of the tibia in patients who have limb-length discrepancy or short stature. *J. Bone. Joint. Surg. Am.* **81**, 624–634 (1999).
31. Tanaka, H. *et al.* Effect of growth hormone therapy in children with achondroplasia: growth pattern, hypothalamic-pituitary function, and genotype. *Eur. J. Endocrinol.* **138**, 275–280 (1998).
32. Kanaka-Gantenbein, C. Present status of the use of growth hormone in short children with bone diseases (diseases of the skeleton). *J. Pediatr. Endocrinol. Metab.* **14**, 17–26 (2001).
33. Scheven, B.A. & Hamilton, N.J. Longitudinal bone growth *in vitro*: effects of insulin-like growth factor I and growth hormone. *Acta Endocrinol.* **124**, 602–607 (1991).
34. Dieudonne, S.C. *et al.* Opposite effects of osteogenic protein and transforming growth factor β on chondrogenesis in cultured long bone rudiments. *J. Bone Miner. Res.* **9**, 771–780 (1994).
35. Coxam, V., Miller, M.A., Bowman, B.M., Qi, D. & Miller, S.C. Insulin-like growth factor 1 and parathyroid hormone effects on the growth of fetal rat metatarsal bones cultured in serum-free medium. *Biol. Neonate.* **68**, 368–376 (1995).
36. Kojima, M., Minamino, N., Kangawa, K. & Matsuo, H. Cloning and sequence analysis of a cDNA encoding a precursor for rat C-type natriuretic peptide (CNP). *FEBS Lett.* **276**, 209–213 (1990).
37. Ogawa, Y. *et al.* Molecular cloning and chromosomal assignment of the mouse C-type natriuretic peptide (CNP) gene (Nppc): comparison with the human CNP gene (NPPC). *Genomics* **24**, 383–387 (1994).
38. Nakayama, H., Yokoi, H. & Fujita, J. Quantification of mRNA by non-radioactive RT-PCR and CCD imaging system. *Nucleic Acids Res.* **20**, 4939 (1992).
39. Yokoi, H. *et al.* Non-radioisotopic quantitative RT-PCR to detect changes in mRNA levels during early mouse embryo development. *Biochem. Biophys. Res. Commun.* **195**, 769–775 (1993).
40. Liu, W. *et al.* Overexpression of Cbfa1 in osteoblasts inhibits osteoblast maturation and causes osteopenia with multiple fractures. *J. Cell. Biol.* **155**, 157–166 (2001).
41. Chusho, H. *et al.* Genetic models reveal that brain natriuretic peptide can signal through different tissue-specific receptor-mediated pathways. *Endocrinology* **141**, 3807–3813 (2000).
42. Mericq, V., Uyeda, J.A., Barnes, K.M., De Luca, F. & Baron, J. Regulation of fetal rat bone growth by C-type natriuretic peptide and cGMP. *Pediatr. Res.* **47**, 189–193 (2000).
43. Bonassar, L.J., Grodzinsky, A.J., Srinivasan, A., Davila, S.G. & Trippel, S.B. Mechanical and physicochemical regulation of the action of insulin-like growth factor-I on articular cartilage. *Arch. Biochem. Biophys.* **379**, 57–63 (2000).
44. Maack, T. *et al.* Physiological role of silent receptors of atrial natriuretic factor. *Science* **238**, 675–678 (1987).

0013-7227/04/$15.00/0
Printed in U.S.A.

Endocrinology 145(2):951–958

doi: 10.1210/en.2003-0816

Androgen Contributes to Gender-Related Cardiac Hypertrophy and Fibrosis in Mice Lacking the Gene Encoding Guanylyl Cyclase-A

YUHAO LI, ICHIRO KISHIMOTO, YOSHIHIKO SAITO, MASAKI HARADA, KOICHIRO KUWAHARA, TAKEHIKO IZUMI, ICHIRO HAMANAKA, NOBUKI TAKAHASHI, RIKA KAWAKAMI, KEIJI TANIMOTO, YASUAKI NAKAGAWA, MICHIO NAKANISHI, YUICHIRO ADACHI, DAVID L. GARBERS, AKIYOSHI FUKAMIZU, AND KAZUWA NAKAO

Department of Medicine and Clinical Science (Y.L., I.K., Y.S., M.H., K.K., T.I., I.H., N.T., R.K., K.T., Y.N., M.N., Y.A., K.N.), Kyoto University Graduate School of Medicine, Kyoto 606-8501, Japan; Howard Hughes Medical Institute and Department of Pharmacology (D.L.G.), University of Texas, Southwestern Medical Center at Dallas, Dallas, Texas 75390; and Center for Tsukuba Advanced Research Alliance (A.F.), Institute of Applied Biochemistry, University of Tsukuba, Tsukuba, Ibaraki 305-8571, Japan

Myocardial hypertrophy and extended cardiac fibrosis are independent risk factors for congestive heart failure and sudden cardiac death. Before age 50, men are at greater risk for cardiovascular disease than age-matched women. In the current studies, we found that cardiac hypertrophy and fibrosis were significantly more pronounced in males compared with females of guanylyl cyclase-A knockout (GC-A KO) mice at 16 wk of age. These gender-related differences were not seen in wild-type mice. In the further studies, either castration (at 10 wk of age) or flutamide, an androgen receptor antagonist, markedly attenuated cardiac hypertrophy and fibrosis in male GC-A KO mice without blood pressure change. In contrast, ovariectomy (at 10 wk of age) had little effect. Also, chronic testosterone infusion increased cardiac mass and fibrosis in ovariectomized GC-A mice. None of the treatments affected cardiac mass or the extent of fibrosis in wild-type mice. Overexpression of mRNAs encoding atrial natriuretic peptide, brain natriuretic peptide, collagens I and III, TGF-β1, TGF-β3, angiotensinogen, and angiotensin converting enzyme in the ventricles of male GC-A KO mice was substantially decreased by castration. The gender differences were virtually abolished by targeted deletion of the angiotensin II type 1A receptor gene (AT1A). Neither castration nor testosterone administration induced any change in the cardiac phenotypes of double-KO mice for GC-A and AT1A. Thus, we suggest that androgens contribute to gender-related differences in cardiac hypertrophy and fibrosis by a mechanism involving AT1A receptors and GC-A. (*Endocrinology* 145: 951–958, 2004)

MYOCARDIAL HYPERTROPHY IS prevalent in a substantial portion of individuals with essential hypertension (1, 2), and it is recognized as an independent risk factor for congestive heart failure and sudden cardiac death (3). Extended cardiac fibrosis results in increased myocardial stiffness, causing ventricular dysfunction and, ultimately, heart failure (4). Significant gender-related differences in the cardiovascular system are now well documented, and before the age of 50, men are at greater risk for cardiovascular diseases than age-matched women (5–9). However, the precise mechanism underlying gender-related differences in cardiac diseases is not fully understood. The results of both *in vitro* and *in vivo* studies indicate that sex steroids play a key role in the development of cardiac structural abnormalities. Estrogen and androgen receptors are present in myocardial tissues (10–12). Estradiol has antiproliferative effects on cardiac fibroblasts (13) and vascular smooth-muscle cells (14, 15), whereas androgens increase proliferation of vascular smooth-muscle cells (16). Studies using sinoaortic denervation-induced cardiac hypertrophy in rats have also shown that testosterone facilitates hypertrophy but estradiol inhibits it (17). A less severe model of cardiac hypertrophy in rats (swimming- or hypertension-induced) failed to confirm the antiproliferative effect of estradiol (18). Moreover, not all males, whether human or experimental animal, develop gender-related cardiac abnormalities. Somjen and colleagues (15) reported a biphasic proliferative response for both estrogen and testosterone in vascular smooth muscle and endothelial cells. It, therefore, is unclear how gender-induced changes in cardiac structural pathology are made manifest.

Mice lacking guanylyl cyclase A (GC-A), a natriuretic peptide receptor, exhibit salt-resistant hypertension, myocardial hypertrophy and interstitial fibrosis, and sudden death (before the age of 6 months) (19–20). In the present study, we found that male GC-A knockout (KO) mice show more pronounced cardiac hypertrophy and fibrosis compared with female GC-A KO mice and that gender-related differences are not seen in wild-type (WT) mice. Additionally, we found that these gender-related differences are attenuated either by castration or flutamide, an androgen receptor (AR) antagonist, and abolished by genetic disruption of angiotensin

Abbreviations: ACE, Angiotensin converting enzyme; Agt, angiotensinogen; Ang, angiotensin; ANP, atrial natriuretic peptide; AR, androgen receptor; AT1A, Ang II type 1A; BNP, brain natriuretic peptide; BW, body weight; GC-A, guanylyl cyclase-A; HR, heart rate; KO, knockout; LVW, left ventricular weight; OVX, ovariectomy; SBP, systolic blood pressure; WT, wild-type.

Endocrinology is published monthly by The Endocrine Society (http://www.endo-society.org), the foremost professional society serving the endocrine community.

(Ang) II type 1A (AT1A) receptors in male GC-A KO mice. We propose that androgens contribute to gender-related differences in cardiac structure and that the AT1A receptor and GC-A are involved in a reciprocal fashion.

Materials and Methods

Animals and treatments

All experimental procedures were carried out in accordance with Kyoto University standards for animal care. GC-A KO mice were originally generated at the University of Texas, Southwestern Medical Center at Dallas and Howard Hughes Medical Institute. Mice were housed in groups of three to five per cage under climate-controlled conditions with a 12-h light/dark cycle and were provided with standard food (CRF-1; Oriental Yeast Co., Ltd, Tokyo, Japan) and water *ad libitum*. The WT (GC-A+/+, AT1A+/+), AT1A KO (GC-A+/+, AT1A−/−), GC-A KO (GC-A−/−, AT1A+/+), and double-KO (GC-A−/−, AT1A−/−) mice used in these experiments were generated from heterozygous (GC-A+/−, AT1A +/−) mice after crossing of single GC-A KO (19) and AT1A KO (21) mice. The genetic background of the original GC-A KO and AT1A KO mice was C57BL/6. Genotypes were determined before and verified after experimentation using PCR. Comparisons of age and body weight (BW) between the KO and WT mice were made among littermates. Also comparisons of age, body weight, and systolic blood pressure (SBP) between control and treated mice were performed.

Measurement of heart rate (HR) and SBP

HR and SBP were measured in conscious mice using a computerized tail-cuff method (Softron Co., Ltd., Tokyo, Japan) (19, 21). Briefly, mice were restrained in a pocket and warmed at 38 C. HR and SBP were measured at 1000–1400 h and calculated as the average of six sessions per day after mice were adapted to the apparatus for 5 d. The validity of this system has been established previously in our laboratory (22).

Measurement of left ventricular weight (LVW) and interstitial fibrosis

After animals were killed by cervical dislocation under anesthesia with ether at 16 wk of age, the hearts were dissected out, LVW was measured, and its ratio to BW (LVW/BW) was calculated and used as an index of ventricular hypertrophy. The left ventricles were then fixed in 10% formalin and prepared for routine histological examination. To determine the degree of collagen fiber accumulation, we randomly selected 20 fields in three individual sections and calculated the ratio of the areas of van Gieson-stained interstitial fibrosis to the total left ventricular area using image analysis software and a Zeiss KS400 system; perivascular fibrosis was excluded in the present study.

mRNA analysis

Total mRNA was prepared from the left ventricle using TRIzol (Life Technologies Inc., Rockville, MD). Expression of mRNAs encoding atrial natriuretic peptide (ANP), brain natriuretic peptide (BNP), collagens I and III, TGF-β1, TGF-β3, angiotensinogen (Agt), and Ang converting enzyme (ACE) was evaluated using quantitative RT-PCR in a 7700 sequence detector (ABI PRISM, Applied Biosystems, Foster City, CA). The oligonucleotide primers are shown in Table 1. Glyceraldehyde-3-phosphate dehydrogenase mRNA was also amplified with specific primers and probe (Applied Biosystems).

Experimental protocols

We first compared the gender-related differences in the phenotypes of 16-wk-old GC-A KO and WT mice (n = 7–9 per group). HR and SBP were measured, and LVW, LVW/BW, and left ventricular fibrosis were calculated, after which related mRNA expression was analyzed.

To evaluate the involvement of estrogen in gender-related differences, we compared the phenotypes of sham-operated and ovariectomized (OVX) mice (n = 7–9 per group). Under anesthesia with ether, the ovaries of 10-wk-old female mice were exteriorized, ligated, and removed *via* bilateral paralumbar incisions, which were then closed with sutures. In sham mice, the ovaries were exteriorized and replaced, and the incisions were closed. Six weeks later, HR and SBP were measured, and the animals were killed.

To investigate the effects of androgens, male mice at 10 wk of age (n = 7–9 per group) were castrated using the trans-scrotal approach. Sham castration consisted of exteriorizing and replacing the testes. As in females, 6 wk later, HR and SBP were measured, and the animals were killed.

To confirm the role of androgen, we ovariectomized female WT and GC-A KO mice (n = 6–7 per group) under anesthesia with ether at 10 wk of age and sc implanted a testosterone pellet (25.0 mg/pellet, 60-darelease, catalog item SA-151) or vehicle pellet (placebo for testosterone, catalog item SC-111) (Innovative Research of America, Sarasota, FL) between the shoulders. Six weeks later, the animals were killed after HR and SBP were measured.

We further confirmed the role of androgens by chronically blocking AR with flutamide (23–24). Flutamide (Sigma Chemical Co., St. Louis, MO; 8 mg/kg·d, dissolved in polyethylene glycol 300) was sc infused for 6 wk using an osmotic mini-pump (model 2002, Alza Corp., Mountain View, CA) at 10 wk of age in male animals (n = 7–9 per group). The mini-pumps were sc implanted under the mice were anesthetized with

TABLE 1. Primer and probe sequences for RT-PCR assays

mRNA	Probe	Primers[a]
ANP	TGTACAGTGCGGTGTCCAACACAGAT	*f*GCCATATTGGAGCAAATCCT
		*r*GCAGGTTCTTGAAATCCATCA
BNP	TGCAGAAGCTGCTGGAGCTGATAAGA	*f*CCAGTCTCCAGAGCAATTCAA
		*r*GCCATTTCCTCCGACTTTT
AT1A	CCGGAATTCAACGCTCCCCA	*f*GTTTGCGCTTTTCATTACGAGT
		*r*TCTTGGTTAGGCCCAGTCCT
ACE	CACATCCCAAACGTGACACCGTACAT	*f*CGGAATGAAACCCATTTTGA
		*r*GCACAAAGCTCACGAAGTACC
Agt	AGGTTCTCAATAGCATCCTCCTCGAACTC	*f*CATTGGTGACACCAACCCC
		*r*GCTGTTCCTCCTCTCCTGCT
TGF-β1	AGCGCATCGAAGCCATCCG	*f*GACGTCACTGGAGTTGTACGG
		*r*GCTGAATCGAAAGCCCTGT
TGF-β3	CGGATGAGCACATAGCCAAGCA	*f*TTGAGCTCTTCCAGATACTTCG
		*r*TTCTTGCCACCTATGTAGCG
Collagen I	CACGGCTGTGTGCGATGACG	*f*GTCCCAACCCCCAAAGAC
		*r*CATCTTCTGAGTTTGGTGATACGT
Collagen III	TCCCACTCTTATTTTGGCACAGCAGTC	*f*TGGTTTCTTCTCACCCTTCTTC
		*r*TGCATCCCAATTCATCTACGT

Sequences are listed 5′ to 3′.
[a] Forward primers are designated by *f* and reverse primers by *r*.

ether and changed with new ones every 2 wk. Control mice were administered only vehicle. Six weeks later, the animals were analyzed.

To assess the involvement of the AT1A receptors in GC-A disruption-induced gender difference, we deleted AT1A receptor by the described method above. At 16 wk of age, the animals (n = 5–9 per group) were analyzed.

To further support the conclusion of AT1A receptor involvement, we castrated male double-KO mice (10 wk old; n = 5–6 per group) and chronically infused exogenous testosterone and analyzed the animals by the described methods above.

Statistical analysis

All results are expressed as means ± SEM. Data were analyzed by one-facter ANOVA. If a statistically significant effect was found, the Newman-Keuls test was performed to isolate the difference between the groups. Values of $P < 0.05$ were considered statistically significant.

Results

GC-A deficiency induces gender-related cardiac differences

Targeted deletion of GC-A led to increased LVW/BW ratios in both male and female mice. However, the effect was greater in males (58% increase *vs.* 33% increase in females; Fig. 1A). In contrast, in WT mice, there was no difference in LVW/BW ratio in males *vs.* females (Fig. 1A). In addition, male GC-A KO mice, but not WT mice, exhibited higher levels of left ventricular fibrosis than did females (378% *vs.* 44%, respectively; Fig. 1, B and C). On the other hand, there was no gender-related difference in HR (WT female 599.6 ± 26.1 *vs.* male 619.0 ± 52.4 beats/min; GC-A KO female 574.5 ± 25.9 *vs.* male 571.3 ± 28.1 beats/min; n = 7–9 per group) or in SBP (WT female 118.4 ± 1.7 *vs.* male 113.2 ± 3.4 mm Hg; GC-A KO female 140.0 ± 3.4 *vs.* male 147.4 ± 2.2 mm Hg; n = 7–9 per group) in either genotype. Male mice weighed more than females, but there was no difference between genotypes [WT female 25.0 ± 0.9 *vs.* male 32.3 ± 1.6 g ($P < 0.05$); GC-A KO female 25.1 ± 0.8 *vs.* male 31.6 ± 1.9 g ($P < 0.05$); n = 7–9 per group].

OVX has little effect in the heart

To elucidate a possible mechanism by which GC-A could prevent gender-related difference in the heart, we first investigated the effects of estrogen depletion. OVX had no effect on HR (WT sham 599.6 ± 26.1 *vs.* OVX 590.4 ± 17.9 beats/min; GC-A KO sham 574.5 ± 25.9 *vs.* OVX 582.3 ± 14.1 beats/min; n = 7–9 per group), SBP (WT sham 118.4 ± 1.7 *vs.* OVX 112.0 ± 2.2 mm Hg; GC-A KO sham 140.6 ± 3.4 *vs.* OVX 137.7 ± 3.0 mm Hg; n = 7–9 per group), LVW/BW ratio, ventricular fibrosis in either mouse type (Fig. 1, A–C), or BW (WT sham 25.0 ± 0.9 *vs.* OVX 25.6 ± 0.8 g; GC-A KO sham 25.1 ± 0.8 *vs.* OVX 25.1 ± 1.6 g; n = 7–9 per group).

Neither castration nor administration of an AR antagonist diminishes cardiac hypertrophy and fibrosis in male GC-A KO mice, whereas testosterone infusion increases cardiac hypertrophy and fibrosis in OVX GC-A mice

In contrast to OVX, removal of testes was associated with a marked reduction in the LVW/BW ratio and in ventricular fibrosis in GC-A KO mice (by 20.5 and 44.7%, respectively) but not to levels comparable to those seen in WT mice. Castration had no effect in WT mice (Fig. 1). Castration reduced BW in male WT as well as in male GC-A KO mice [WT 5.7 ± 0.5 *vs.* 2.1 ± 0.4 g ($P < 0.05$), and GC-A KO 6.6 ± 0.9 *vs.* 2.7 ± 0.6 g ($P < 0.05$) for sham and castrated groups, respectively; n = 7–9 per group]. Castration had no effect on HR (WT 619.0 ± 52.4 *vs.* 606.2 ± 45.9 beats/min, and GC-A KO 571.3 ± 28.1 *vs.* 600.2 ± 13.2 beats/min, for sham and castrated groups, respectively; n = 7–9 per group) or SBP

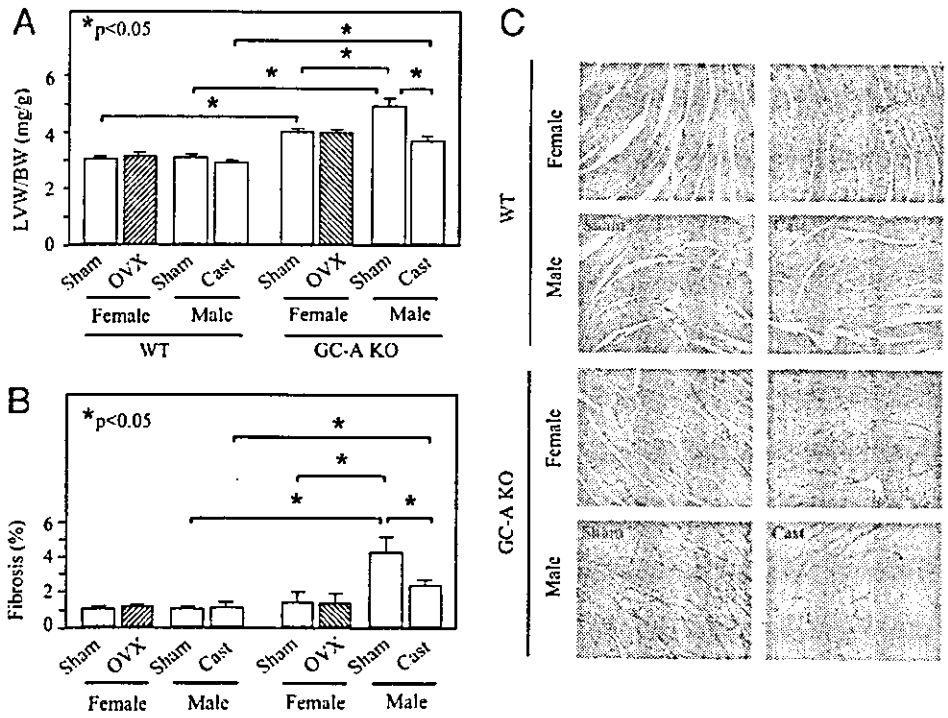

FIG. 1. GC-A disruption-induced gender-related differences in cardiac hypertrophy and fibrosis were inhibited by castration in male (Cast), but not in female (OVX) mice that were castrated at 10 wk and analyzed at 16 wk of age. The ratio of the areas of van Gieson-stained interstitial fibrosis to the total left ventricular area was calculated using image analysis software and a Zeiss KS400 system. A, LVW/BW ratio; B, relative levels of left ventricular fibrosis; C, photomicrographs showing representative examples of cardiac fibrosis (red) (magnification, ×200). Values are means ± SEM; n = 7–9 per group; *, $P < 0.05$.

(WT 113.2 ± 3.4 *vs.* 105.8 ± 4.2 mm Hg, and GC-A KO 147.4 ± 2.2 *vs.* 142.2 ± 6.3 mm Hg, for sham and castrated groups, respectively; n = 7–9 per group). The AR antagonist flutamide had similar effects to castration on LVW/BW, fibrosis (Fig. 2), HR (data not shown), and SBP (data not shown). In contrast, chronic infusion of testosterone increased LVW/BW ratio (by 20%) and cardiac fibrosis (by 114%) in OVX GC-A mice but not in OVX WT mice (Fig. 3). Testosterone treatment was also associated with increased BW in GC-A KO but not in WT mice]WT 2.6 ± 0.3 *vs.* 3.2 ± 0.3 g ($P < 0.05$), and GC-A KO 2.9 ± 0.2 *vs.* 5.2 ± 0.5 g ($P < 0.05$), for sham and testosterone-treated groups, respectively; n = 6–9 in each group[. HR and SBP were not affected by testosterone treatment (data not shown).

Gender-related difference in molecular expression profile

Basal left ventricular levels of ANP, BNP, collagen I, collagen III, TGF-β1, and TGF-β3 mRNAs were all higher in male than female GC-A KO mice. Castration of males decreased mRNA expression of these molecules to levels seen in females (Fig. 4). Again, no gender-related difference or castration-associated effects were seen in WT mice (Fig. 4). In contrast to the above mentioned genes, the levels of Agt and ACE mRNAs were higher in males than in females, and castration of males strongly suppressed their expression, and their levels were comparable in both genotypes of mice.

Deletion of AT1A abolishes gender-related cardiac differences

Deletion of the AT1A gene in GC-A KO mice reduced LVW/BW in both male and female mice, but the effects were more pronounced in the males (by 34 and 32.7% in males *vs.* 18 and 23.5% in females, respectively). AT1A deletion also markedly reduced cardiac fibrosis in male GC-A KO mice (by 57.5%). Gender-related cardiac differences (LVW/BW and fibrosis) were evident only in GC-A KO mice, but not in WT (as above), AT1A KO or double-KO mice (Fig. 5).

Castration or testosterone infusion fails to induce changes in cardiac mass and fibrosis in male double-KO mice

In contrast to the data obtained in GC-A KO mice (see above), neither castration nor testosterone infusion affected cardiac mass or the level of fibrosis in male double-KO mice (data not shown). Similarly, HR and SBP were unaffected by either castration or testosterone replacement (data not shown).

Discussion

As previous literatures documented significant gender-related differences in cardiovascular function and geometry (6, 7), the present study demonstrates that male GC-A KO mice show more marked left ventricular hypertrophy and severe interstitial fibrosis than female ones. Considering the protective effects of estrogen on the cardiovascular system (25, 26), we first investigated the effects of estrogens on the gender-related difference in the GC-A KO mouse hearts. Although OVX had little effect on cardiac mass and fibrosis in both WT and GC-A KO mice, there are still some possibilities that have not been addressed, such as, first, the fact that the effects of estrogen deprivation in women are not immediate; they develop over years, meaning that the 6-wk period of estrogen deprivation may be insufficient. Second, phytoestrogens are found in over 300 plants, including some used in human and animal diets (27–29). They can bind to the estrogen receptor and induce estrogen-like effects in animals, humans, and cells in culture. In the present study, we cannot exclude the possibility that the chow of mice may contain phytoestrogens, which may protect from (or limit) the effects of OVX. Therefore, the role of estrogen in gender-related cardiac difference observed in GC-A KO mice should be further clarified.

Next, we examined the effects of androgens. ARs are widely distributed in the cardiovascular system, where they have been identified on aortic, peripheral vascular, ventricular, and atrial myocytes (30), and were recently shown to mediate robust, testosterone-induced hypertrophic responses in cardiac myocytes (12). Nevertheless, although virtually all men have much higher levels of androgens than women do, not all men exhibit more severe cardiac hypertrophy and fibrosis. In the present study, significant gender-related differences in cardiac abnormalities were observed only in GC-A KO mice. In addition, it is notable that both castration and AR antagonist markedly diminished cardiac hypertrophy and fibrosis in male GC-A KO mice, and chronic

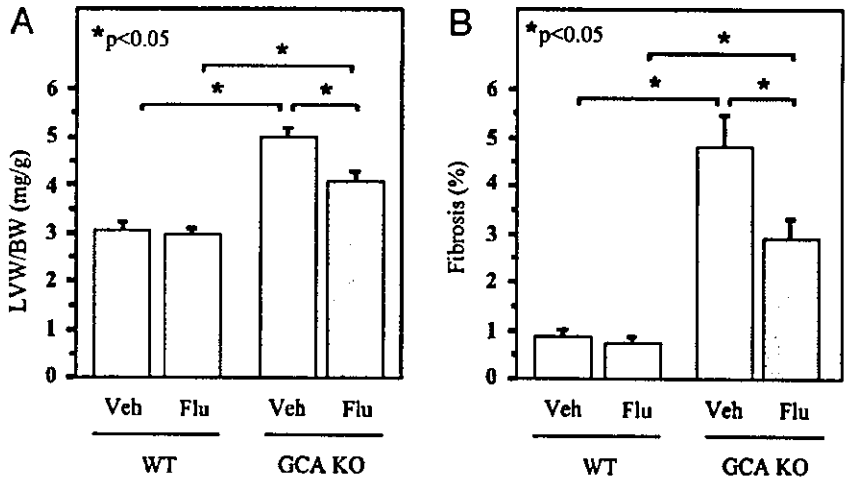

FIG. 2. Chronic AR blockade with flutamide was associated with decreased LVW/BW (A) and left ventricular fibrosis (B) in male GC-A KO mice. Flutamide (Flu; 8 mg/kg·d) or vehicle (Veh) was sc infused for 6 wk starting at 10 wk of age. Values are mean ± SEM; n = 7–9 per group; *, $P < 0.05$.

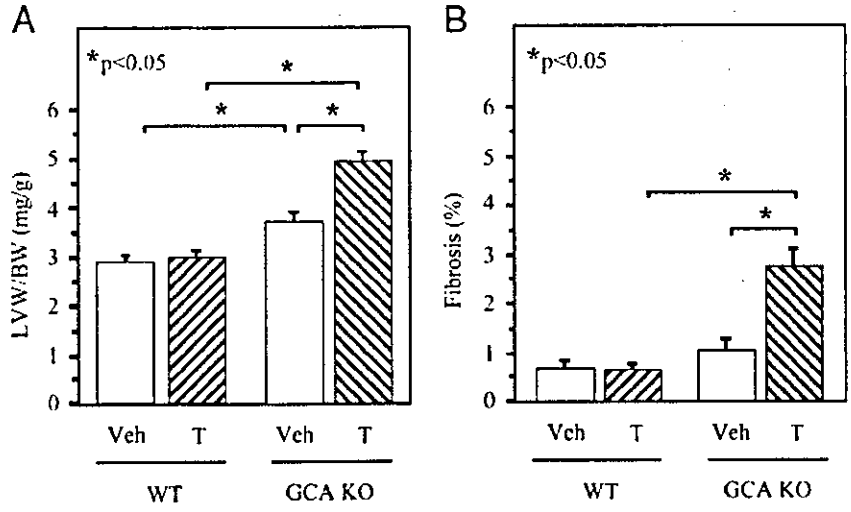

FIG. 3. Chronic infusion of testosterone (T) was associated with an increased LVW/BW (A) and left ventricular fibrosis (B) in OVX GC-A KO but not in OVX WT mice. A testosterone pellet (25.0 mg/pellet) or vehicle (Veh) was implanted sc at 10 wk of age, and 6 wk later, the animals were killed and analyses performed. Values are mean ± SEM; n = 6–7 per group; *, $P < 0.05$.

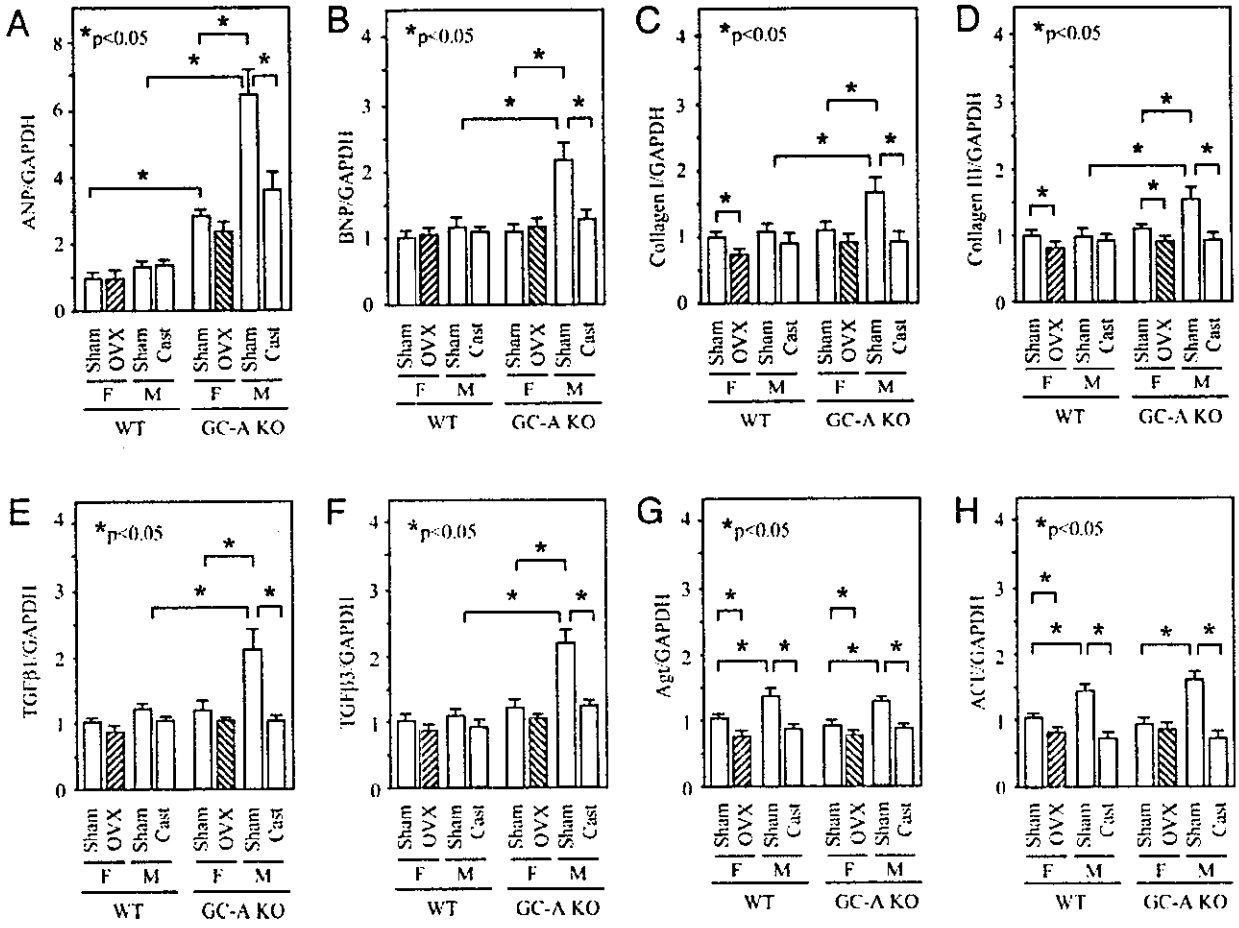

FIG. 4. Left ventricular levels of ANP, BNP, collagen I, collagen III, TGF-β1, and TGF-β3 mRNAs were elevated in male (M) GC-A KO mice and were reduced by castration to levels seen in females (F). Enhanced levels of Agt and ACE expression in male WT and GC-A KO mice were suppressed by castration, and levels were comparable in both genotypes. mRNAs were evaluated using quantitative RT-PCR in a 7700 sequence detector (ABI PRISM). Levels in sham female WT mice were arbitrarily assigned a value of 1.0. A, ANP; B, BNP; C, collagen I; D, collagen III; E, TGF-β1; F, TGF-β3; G, Agt; H, ACE. Values are mean ± SEM; n = 7–9; *, $P < 0.05$.

testosterone infusion increased cardiac mass and fibrosis only in OVX GC-A KO mice. ANP and BNP are well established molecular markers for cardiac hypertrophy. It has been demonstrated that the testosterone metabolite dihydrotestosterone is able to increase ANP secretion from ventricular myocytes. An AR antagonist, cyproterone, abolished

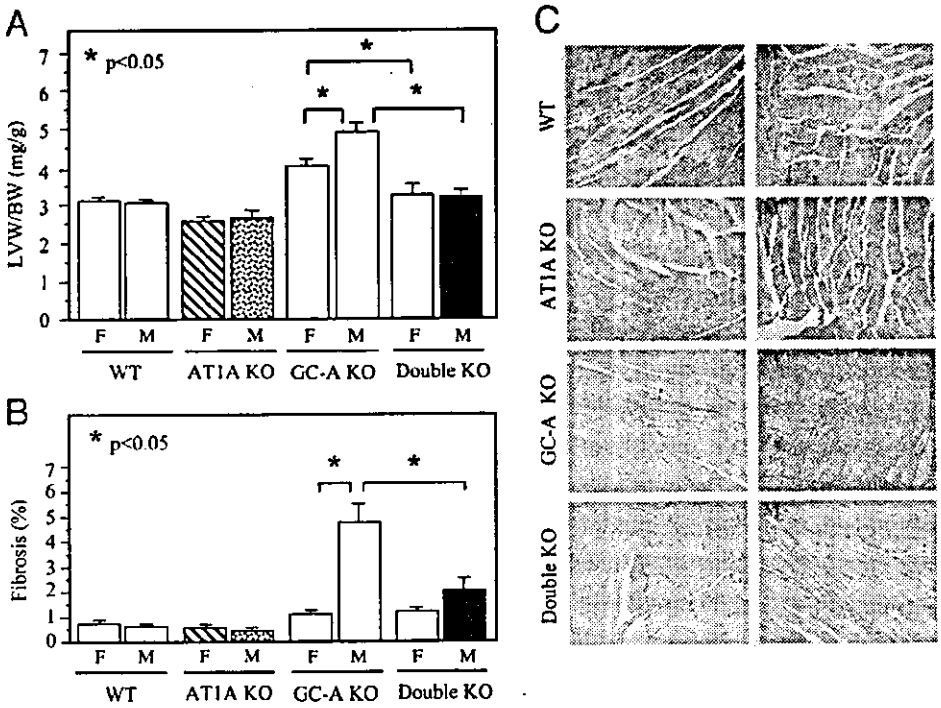

FIG. 5. Deletion of the AT1A receptor gene abolishes the gender-related differences in LVW/BW (A) and the relative levels of left ventricular fibrosis (B). C, Representative photomicrographs demonstrating fibrosis (red) in GC-A KO mice. Animals were analyzed at 16 wk of age. Values are mean ± SEM; n = 5–9 per group; *, $P < 0.05$.

this effect (12). Like cardiac geometric changes, changes in ANP and BNP, or markers for ventricular fibrosis, collagen I, and collagen III were higher in male GC-A KO mice than in females and were reduced by removal of testes. These findings suggest that androgens play an important role in gender-related cardiac differences in GC-A KO mice. Castration in males and AR antagonist could not reduce the cardiac mass and fibrosis to WT levels, suggesting that more than androgens are involved.

Ang II is known to potently stimulate cardiomyocyte and fibroblast growth, both *in vitro* and *in vivo* (31, 32), and the tissue renin-Ang system is known to play a key role in cardiac remodeling (33). It has been proposed that increased ACE abundance in the hypertrophied and failing heart may contribute to the local generation of Ang II and impact cardiac remodeling through local paracrine or autocrine effects (34–36). The greater abundance of ventricular ACE in males may contribute to the tendency of male rodents to develop cardiac abnormalities, which has been described in transgenic mouse models (37, 38) and spontaneously hypertensive rats (39) and in response to left ventricular pressure overload in rats (10) and in humans (40–42). It has been reported that hepatic Agt mRNA levels are higher in intact male hypertensive rats than in the females; moreover, those levels are reduced by orchidectomy and increased by administration of testosterone (43). Recently, Freshour *et al.* (44) demonstrated a gender difference in the expression of ACE in the murine heart with greater cardiac ACE levels seen in male animals compared with females. Moreover, ventricular ACE levels were substantially decreased in androgen-deprived males (44). Consistent with those reports, our data show that levels of cardiac Agt and ACE expression are higher in the ventricles of both GC-A KO and WT males than they are in females. Castration reduced expression of Agt in the male ventricle to levels approximating those seen in the females in both WT and GC-A KO mice. Given the evidence that Ang II has hypertrophic and fibrogenic activities in the heart, Ang II is a possible candidate to link androgens with cardiac abnormalities. It should be noted, however, that gender-related increases in LVW/BW ratios and interstitial fibrosis were observed only in the GC-A KO mice but not in WT mice, despite the similar up-regulation of Agt and ACE expression in ventricles of both genotypes of mice. We recently observed that GC-A signaling counteracts Ang II-induced cardiac abnormalities. A subpressor dose of Ang II increased cardiac mass and fibrosis only in male GC-A KO but not WT mice, suggesting an augmented responsiveness to Ang II in the heart of GC-A KO mice (22). Thus, we speculate that gender-related differences in the heart were made manifest by lacking inhibitory actions of GC-A on AT1 signaling in GC-A KO mice. Inhibitory effects of GC-A were also supported by the overexpression of TGF-β1 and -β3, which are activated by AT1A signaling and responsible for interstitial fibrosis (28, 45–47), in GC-A KO mice.

To further test this hypothesis, we deleted the AT1A receptor gene, which mediates classical Ang II actions, including cardiac hypertrophy and fibrosis, by crossing GC-A KO mice and AT1A KO mice. The gender-related cardiac differences were absent in the double-KO mice. Furthermore, castration of males did not reduce and testosterone administration failed to increase the cardiac mass and fibrosis in male double-KO mice. These results strongly suggest that GC-A prevents androgen-induced cardiac abnormalities mainly by inhibiting the androgen-Ang II-AT1A axis.

The present data did not indicate that androgens and Ang II solely provide a causative contribution to gender-related cardiac differences in GC-A KO mice. LVW/BW in male GC-A KO mice after castration or flutamide treatment were

comparable to that in female GC-A KO mice, but the degree of fibrosis was still higher in male GC-A KO mice after the treatments than in females, suggesting androgens mostly contribute to gender-related left ventricular hypertrophy, and at least approximately 50% to the gender-related increase in fibrosis. In the case of AT1A blockade, LVW/BW in GC-A KO mice were reduced to the level corresponding to that in WT mice, in which there was no difference in hypertrophy, and fibrosis was more intensively reduced by knocking out the AT1A receptor, compared with blockade of ARs. These findings suggest that AT1A signaling contributes not only to gender-related cardiac abnormalities but also to abnormalities specifically observed in both genders of GC-A KO mice, suggesting androgen is one of the factors up-regulating the Ang system. Additional studies are required to elucidate the entire mechanism for gender-related difference observed in GC-A KO mice, in which other molecules, such as catecholamines and endothelin, would be involved.

Another interesting finding is that castration or the treatment with androgen antagonist improved cardiac abnormalities in GC-A KO mice without significant change in SBP. As mentioned above, a subpressor dose of Ang II exaggerated hypertrophy and fibrosis in GC-A KO mice (22). It is likely, therefore, that androgen-induced Ang II is sufficient for inducing hypertrophy and fibrosis in GC-A KO mice but not to elevate BP.

The presence or absence of androgens in male GC-A KO mice showed marked effects on the expression levels of ANP. The molecular mechanism is unclear at present. In the present study, despite the similar up-regulation of Agt and ACE expression in ventricles of both male WT and GC-A KO mice, ANP was markedly increased only in male GC-A KO mice. We demonstrated a similar expression level of AT1A mRNA in males and females of both WT and GC-A KO mice (data not shown). Therefore, it seems that androgen-induced intracellular signaling at a postreceptor level for modulation of ANP gene expression is up-regulated in GC-A KO mice. Ang II is known to increase ANP expression mediated by protein kinase C or MAPK (48). Further examination is necessary to determine whether the protein kinase C or MAPK pathway is involved in the elevation of ANP by androgens.

Recently, Nakayama *et al.* (49) described a functional mutation in the 5′-flanking region of the human GC-A gene that reduces transcriptional activity by more than 70% in reporter gene assay, is present in approximately 5% of the hypertensive individuals in Japan, and is associated with cardiac hypertrophy. Evidence also suggests that GC-A receptors may be down-regulated in patients with chronic, severe heart failure (50). Indeed, there may be substantial numbers of patients whose abnormal GC-A signaling makes them susceptible to androgen-induced cardiac abnormalities. From the clinical points of view, the present study raises the possibility of the prophylactic use of Ang II receptor blocker or AR antagonist in patients with loss of functional mutations in the GC-A gene.

Taken together, our findings strongly support the hypothesis that androgen contributes to cardiac abnormalities *via* the AT1A receptor. Furthermore, this androgenic effect is normally inhibited by stimulation of GC-A by natriuretic peptides.

Acknowledgments

We thank Ms. Makoto Mukai and Ms. Itone Makino for their excellent secretarial assistance and Ms. Mika Inoue for her technical assistance. Dr. Yuhao Li is a foreign research fellow of the Japan Society for the Promotion of Science.

Received June 30, 2003. Accepted October 22, 2003.

Address all correspondence and requests for reprints to: Yoshihiko Saito, First Department of Internal Medicine, Nara Medical University, 840, Shijo-cho, Kashihara, Nara 634-8522, Japan. E-mail: yssaito@naramed-u.ac.jp.

This work was supported in part by research grants from Japanese Ministry of Education, Science and Culture, the Japanese Ministry of Health and Welfare, the Japanese Society for the Promotion of Science Research for the Future program (JSPS-RFTF96I00204 and JSPS-RFTF98L00801), the Uehara Memorial Foundation, the Smoking Research Foundation, and the Howard Hughes Medical Institute.

References

1. **Devereux RB, Pickering TG, Alderman MH, Chien S, Borer JS, Laragh JH** 1987 Left ventricular hypertrophy in hypertension: prevalence and relationship to pathophysiologic variables. Hypertension 9(Suppl II):53–60
2. **Kaplinsky E** 1994 Significance of left ventricular hypertrophy in cardiovascular morbidity and mortality. Cardiovasc Drugs Ther 8:549–556
3. **Neyses L, Pelzer T** 1995 The biological cascade leading to cardiac hypertrophy. Eur Heart J 16(Suppl N):8–11
4. **Weber KT, Brilla CG** 1991 Pathological hypertrophy and cardiac interstitium. Fibrosis and renin-angiotensin-aldosterone system. Circulation 83:1849–1865
5. **Hayward CS, Kelly RP, Collins P** 2000 The roles of gender, the menopause and hormone replacement on cardiovascular function. Cardiovasc Res 46: 28–49
6. **Fiebach NH, Viscoli CM, Horwitz RI** 1990 Differences between women and men in survival after myocardial infarction. JAMA 263:1092–1096
7. **de Simone G, Devereux RB, Daniels SR, Meyer RA** 1995 Gender differences in ventricular growth. Hypertension 26:979–983
8. **Luchner A, Brockel U, Muscholl M, Hense HW, Doring A, Riegger GA, Schunkert H** 2002 Gender-specific differences of cardiac remodeling in subjects with left ventricular dysfunction: a population-based study. Cardiovasc Res 53:720–727
9. **Crabbe DL, Dipla K, Ambati S, Zafeiridis A, Gaughan JP, Houser SR, Margulies KB** 2003 Gender differences in post-infarction hypertrophy in end-stage failing hearts. J Am Coll Cardiol 41:300–306
10. **Weinberg EO, Thienelt CD, Katz SE, Bartunek J, Tajima M, Rohrbach S, Douglas PS, Lorell BH** 1999 Gender differences in molecular remodeling in pressure overload hypertrophy. J Am Coll Cardiol 34:264–273
11. **Meyer R, Linz KW, Surges R, Meinardus S, Vees J, Hoffmann A, Windholz O, Grohe C** 1998 Rapid modulation of L-type calcium current by acutely applied oestrogens in isolated cardiac myocytes from human, guinea-pig and rat. Exp Physiol 83:305–321
12. **Marsh JD, Lehmann MH, Ritchie RH, Gwathmey JK, Green GE, Schiebinger RJ** 1998 Androgen receptors mediate hypertrophy in cardiac myocytes. Circulation 98:256–261
13. **Dubey RK, Gillespie DC, Jackson EK, Keller PJ** 1998 17β-Estradiol, its metabolites, and progesterone inhibit cardiac fibroblast growth. Hypertension 31:522–528
14. **Chen SJ, Li H, Durand J, Oparil S, Chen YF** 1996 estrogen reduces myointimal proliferation after balloon injury of rat carotid artery. Circulation 93:577–584
15. **Somjen D, Kohen F, Jaffe A, Amir-Zaltsman Y, Knoll E, Stern N** 1998 Effect of gonadal steroids and their antagonists on DNA synthesis in human vascular cells. Hypertension 32:39–45
16. **Fujimoto R, Morimoto I, Morita E, Sugimoto H, Ito Y, Eto S** 1994 Androgen receptors, 5α-reductase activity and androgen-dependent proliferation of vascular smooth muscle cells. J Steroid Biochem Mol Biol 50:169–174
17. **Cabral AM, Vasquez EC, Moyses MR, Antonio A** 1988 Sex hormone modulation of ventricular hypertrophy in sinoaortic denervated rats. Hypertension 11:193–197
18. **Malhotra A, Buttrick P, Scheuer J** 1990 Effects of sex hormones on development of physiological and pathological cardiac hypertrophy in male and female rats. Am J Physiol 259:H866–H871
19. **Lopez MJ, Wong SK, Kishimoto I, Dubois S, Mach V, Friesen J, Garbers DL, Beuve A** 1995 Salt-resistant hypertension in mice lacking the guanylyl cyclase-A receptor for atrial natriuretic peptide. Nature 378:65–68
20. **Oliver PM, Fox JE, Kim R, Rockman HA, Kim HS, Reddick RL, Pandey KN, Milgram SL, Smithies O, Maeda N** 1997 Hypertension, cardiac hypertrophy, and sudden death in mice lacking natriuretic peptide receptor A. Proc Natl Acad Sci USA 94:14731–14735
21. **Sugaya T, Nishimatsu S, Tanimoto K, Takimoto E, Yamagishi T, Imamura K, Goto S, Imaizumi K, Hisada Y, Otsuka A, Uchida H, Sugiura M, Fukuta**

K, Fukamizu A, Murakami K 1995 Angiotensin II type 1a receptor-deficient mice with hypotension and hyperreninemia. J Biol Chem 270:18719–18722
22. Li Y, Kishimoto I, Saito Y, Harada M, Kuwahara K, Izumi T, Takahashi N, Kawakami R, Tanimoto K, Nakagawa Y, Nakanishi M, Adachi Y, Garbers DL, Fukamizu A, Nakao K 2002 Guanylyl cyclase-A inhibits angiotensin II type 1A receptor-mediated cardiac remodeling, an endogenous protective mechanism in the heart. Circulation 106:1722–1728
23. Labrie F 1993 Mechanisms of action and pure antiandrogenic properties of flutamide. Cancer 72:3816–3827
24. Reckelhoff JF, Zhang H, Srivastava K, Granger JP 1999 Gender differences in hypertension in spontaneously hypertensive rats: role of androgens and androgen receptor. Hypertension 34:920–923
25. Mendelsohn ME, Karas RH 1999 The protective effects of estrogen on the cardiovascular system. N Engl J Med 340:1801–1811
26. van Eickels M, Grohe C, Cleutjens JP, Janssen BJ, Wellens HJ, Doevendans PA 2001 17β-Estradiol attenuates the development of pressure-overload hypertrophy. Circulation 104:1419–1423
27. Farnsworth NR, Bingel AS, Cordell GA, Crane FA, Fong HHS 1975 Potential value of plants as sources of new antifertility agents. J Pharm Sci 64:717–754
28. Price KR, Fenwick GR 1985 Naturally occurring oestrogens in foods: a review. Food Addit Contam 2:73–106
29. Degen GH, Janning P, Diel P, Bolt HM 2002 Estrogenic isoflavones in rodent diets. Toxicol Lett 128:145–157
30. Mcgill HC, Sheridan PJ 1981 Nuclear uptake of sex steroid hormones in the cardiovascular system of the baboon. Circ Res 48:238–244
31. Sadoshima J, Izumo S 1993 Molecular characterization of angiotensin II-induced hypertrophy of cardiac myocytes and hyperplasia of cardiac fibroblasts. Critical role of AT1 receptor subtype. Circ Res 73:413–423
32. Schorb W, Booz GW, Dostal DE, Conrad KM, Chang KC, Baker KM 1993 Angiotensin II is mitogenic in neonatal rat cardiac fibroblasts. Circ Res 72: 1245–1254
33. McDonald KM, Garr M, Carlyle PF, Francis GS, Hauer K, Hunter DW, Parish T, Stillman A, Cohn JN 1999 Relative effects of α1-adrenergic blockade, converting enzyme inhibitor therapy, and angiotensin II subtype 1 receptor blockade on ventricular remodeling in the dog. Circulation 90:3034–3046
34. Bader M, Peters J, Baltatu O, Muller DN, Luft FC, Ganten D 2001 Tissue rennin-angiotensin systems: new insights from experimental animal models in hypertensive research. J Mol Med 79:76–102
35. Pratt RE 1999 Angiotensin II and the control of cardiovascular structure. J Am Soc Nephrol 10:S120–S128
36. Weber KT 1997 Extra cellular matrix remodeling in heart failure. A role for de novo angiotensin II generation. Circulation 96:4065–4082
37. Kadokami T, McTiernan CF, Kubota T, Frye CS, Feldman AM 2000 Sex-related survival differences in murine cardiomyopathy are associated with differences in TNF-receptor expression. J Clin Invest 106:589–597
38. Vikstrom KL, Factor SM, Leinwand LA 1996 Mice expressing mutant myosin are a model for hypertrophic cardiomyopathy. Mol Med 2:556–567
39. Wallen WJ, Cserti C, Belanger MP, Wittnich C 2000 Gender-differences in myocardial adaptation to afterload in normotensive and hypertensive rats. Hypertension 36:774–779
40. Carroll JD, Carroll EP, Feldman T, Ward DM, Lang RM, McGaughey D, Karp RB 1992 Sex-associated differences in left ventricular function in aortic stenosis of the elderly. Circulation 86:1099–1107
41. Douglas PS, Katz SE, Weinberg EO, Chen MH, Bishop SP, Lorell BH 1998 Hypertrophic remodeling: gender differences in the early response to left ventricular pressure overload. J Am Coll Cardiol 32:1118–1125
42. Villarreal FJ, Dillmann WH 1992 Cardiac hypertrophy-induced changes in mRNA levels for TGF-β1, fibronectin, and collagen. Am J Physiol Heart Circ Physiol 262:H1861–H1866
43. Chen YF, Naftilan AJ, Oparil S 1992 Androgen-dependent angiotensinogen and renin messenger RNA expression in hypertensive rats. Hypertension 19:456–463
44. Freshour JR, Chase SE, Vikstrom KL 2002 Gender differences in cardiac ACE expression are normalized in androgen-deprived male mice. Am J Physiol Heart Circ Physiol 283:H1997–H2003
45. Border WA, Nobel NA 1994 Transforming growth factor-β in tissue fibrosis. N Engl J Med 331:1286–1292
46. Kagami S, Border WA, Miller DE, Noble NA 1994 Angiotensin II stimulates extracellular matrix protein synthesis through induction of transforming growth factor-β expression in rat glomerular mesangial cells. J Clin Invest 93:2431–2437
47. Johnston CI, Hodsman PG, Kohzuki M, Casley DJ, Fabris B, Phillips PA 1989 Interaction between atrial natriuretic peptide and the renin angiotensin aldosterone system. Am J Med 87:24S–28S
48. Sadoshima J, Izumo S 1997 The cellular and molecular response of cardiac myocytes to mechanical stress. Annu Rev Physiol 59:551–571
49. Nakayama T, Soma M, Takahashi Y, Rehemudula D, Kanmatsuse K, Furuya K 2000 Functional deletion mutation of the 5′-flanking region of type A human natriuretic peptide receptor gene and its association with essential hypertension and left ventricular hypertrophy in the Japanese. Circ Res 86:841–845
50. Tsutamoto T, Kanamori T, Morigami N, Sugimoto Y, Yamaoka O, Kinoshita M 1993 Possibility of down-regulation of atrial natriuretic peptide receptor coupled to guanylate cyclase in peripheral vascular beds of patients with chronic severe heart failure. Circulation 88:811–813

Endocrinology is published monthly by The Endocrine Society (http://www.endo-society.org), the foremost professional society serving the endocrine community.

Plasma Level of B-Type Natriuretic Peptide as a Prognostic Marker After Acute Myocardial Infarction

A Long-Term Follow-Up Analysis

Satoru Suzuki, MD; Michihiro Yoshimura, MD; Masafumi Nakayama, MD; Yuji Mizuno, MD; Eisaku Harada, MD; Teruhiko Ito, MD; Shota Nakamura, MD; Koji Abe, MD; Megumi Yamamuro, MD; Tomohiro Sakamoto, MD; Yoshihiko Saito, MD; Kazuwa Nakao, MD; Hirofumi Yasue, MD; Hisao Ogawa, MD

Background—Circulating levels of B-type natriuretic peptide (BNP), a cardiac hormone, reflect the severity of cardiac dysfunction. Because the plasma BNP level changes dramatically during the period after the onset of acute myocardial infarction (AMI), identification of a suitable sampling time is problematic. There have been several reports indicating that the plasma BNP level obtained in the acute phase of AMI can be used as a prognostic marker. We examined whether the plasma BNP level measured 3 to 4 weeks after the onset of AMI represents a reliable prognostic marker for patients with AMI.

Methods and Results—We analyzed 145 consecutive patients with AMI. Plasma BNP levels were measured during the 3 to 4 weeks after onset of AMI. Of those patients, 23 experienced fatal cardiac events during this study. The mean follow-up period was 58.6 months. Log BNP, left ventricular end-diastolic pressure, and pulmonary vascular resistance were all significantly higher in the cardiac death group, and there were more men and more patients with a history of heart failure in the cardiac death group. A Cox proportional hazards model analysis showed that log BNP was an independent predictor of cardiac death. The survival rate was significantly higher in patients with log BNP <2.26 (180 pg/mL) than in those with log BNP ≥ 2.26.

Conclusions—The plasma BNP level obtained 3 to 4 weeks after the onset of AMI can be used as an independent predictor of cardiac death in patients with AMI. (***Circulation.*** **2004;110:1387-1391.)**

Key Words: natriuretic peptides ■ myocardial infarction ■ prognosis

B-type natriuretic peptide (BNP) is a cardiac hormone that is secreted mainly from the ventricles; it has many biological effects, including vasodilation, natriuresis, and inhibition of both the rennin-angiotensin and sympathetic nervous systems.[1–7] BNP is secreted from the failing heart into the systemic circulation; the plasma level of this peptide is elevated in patients with heart failure.[8–11] The plasma BNP level has been recognized as a biochemical marker of ventricular dysfunction.[9–15]

We previously reported that the plasma BNP level increases rapidly and markedly just after the onset of acute myocardial infarction (AMI).[13,16] The plasma level of BNP changes dramatically in some patients. The time course of the plasma BNP level could be divided into 2 patterns after the onset of AMI: a biphasic pattern with 2 peaks and a monophasic pattern with 1 peak. There were significantly more patients with anterior infarction, congestive heart failure, a higher maximum level of creatine kinase-MB isoenzyme, and a lower left ventricular ejection fraction in the biphasic group than in the monophasic group; this suggests that the biphasic pattern reflects the degree of left ventricular dysfunction or the size of the infarct.[13]

The mechanism for the formation of the first plasma BNP peak was shown to be due to the genetic characteristics of BNP: The DNA of BNP has an AT-rich sequence in the 3′-untranslated region, which destabilizes mRNA.[12,17] For this reason, BNP is considered to be an acute-phase reactant in response to acute tissue injuries.[12,13,17,18] Hemodynamic parameters, as well as some humoral factors such as interleukin-1β, endothelin-1, and angiotensin II, induce secretion of BNP in the early phase of AMI, thus accounting for the first peak.[13,19–22] The mechanisms for the formation of the

Received January 16, 2004; de novo received March 30, 2004; revision received May 4, 2004; accepted May 6, 2004.

From the Department of Cardiovascular Medicine (S.S., M. Yoshimura, M.N., S.N., K.A., M. Yamamuro, T.S., H.O.), Graduate School of Medical Sciences, Kumamoto University, Kumamoto, Japan; Division of Cardiology (Y.M., E.H., T.I., H.Y.), Kumamoto Aging Research Institute, Kumamoto, Japan; First Department of Internal Medicine (Y.S.), Nara Medical University, Nara, Japan; and Department of Medicine and Clinical Science (K.N.), Kyoto University Graduate School of Medicine, Kyoto, Japan.

Reprint requests to Michihiro Yoshimura, Department of Cardiovascular Medicine, Graduate School of Medical Sciences, Kumamoto University, 1-1-1 Honjo, Kumamoto 860-8556, Japan. E-mail bnp@kumamoto-u.ac.jp

Circulation is available at http://www.circulationaha.org

DOI: 10.1161/01.CIR.0000141295.60857.30

second peak are considered to be related to infarct expansion and subsequent ventricular remodeling.[12,13]

As mentioned above, the changing pattern of the plasma BNP level varies according to the cardiac condition after AMI. This raises the possibility that the plasma BNP level could reflect or predict prognosis after the onset of AMI. The changing pattern of the plasma BNP level after the onset of AMI is dynamic during the first month; therefore, identification of a suitable time frame for blood sampling for BNP measurement is an important issue. To exploit the plasma BNP level as a clinically useful prognostic marker after AMI in the future, it would be convenient to measure it 3 to 4 weeks after the onset of AMI. It is generally difficult to target the timing of the blood sampling to the formation of the second plasma BNP peak, although this strict time point may be better as a prognostic marker than the later phase, such as 3 to 4 weeks after the onset. According to our previous study, the plasma BNP level was still significantly higher in patients with the biphasic pattern than in those with the monophasic pattern at 3 to 4 weeks after onset of AMI,[13] which suggests that sampling at this time would also be valuable for clinical use. In the present study, we examined whether the plasma BNP level measured 3 to 4 weeks after the onset of AMI represents a reliable prognostic marker after AMI by monitoring patients with AMI for a long-term period. The present study began just after the discovery of BNP, and therefore we were able to monitor the patients for ≈5 years on average and as long as 13 years.

Methods

Study Patients

This study began in January 1990, just after the discovery of BNP, and an antibody for BNP was established by our research group.[9,23,24] The end of the patient recruitment period was in March 1999. The final follow-up date was on May 31, 2003. During this time period, there were 403 admitted patients with AMI who underwent cardiac catheterization and in whom we were able to measure the plasma BNP level 3 to 4 weeks after the onset of AMI. We followed up 285 patients and were ultimately able to follow up 145 patients with highly reliable information about their prognosis from themselves, their families, and/or their affiliated hospitals. The 145 study patients consisted of 106 men and 39 women with a mean age of 65.1 years (range 31 to 90 years).

The diagnosis of AMI was made from clinical symptoms, including chest pain, ECG changes including ST elevation and ST depression, and an elevation of serum creatine kinase-MB isoenzyme to more than twice the normal upper level. In the present study, we defined the cardiac death group as patients who died of heart failure or sudden cardiac death and the non-cardiac-death group as survivors, including patients who died of causes other than cardiac events. The protocol was in agreement with the guidelines of the ethics committee at our institution, and written informed consent was obtained from each patient before they were enrolled in the study.

Cardiac Catheterization

Cardiac catheterization was performed in 145 patients at 3 to 4 weeks after AMI. A Swan-Ganz catheter was inserted into the femoral or subclavian vein, and hemodynamic measurements were obtained, including pulmonary capillary wedge pressure, pulmonary artery pressure, right atrial pressure, and cardiac output. Cardiac output was determined in triplicate by the thermodilution technique. Blood samples that included BNP were obtained from either the femoral or subclavian vein.

After the Swan-Ganz catheterization procedure, aortic pressure and left ventricular end-diastolic pressure were measured; then, coronary angiography and left ventriculography were performed. The left ventricular ejection fraction was determined by left ventriculography.

Measurement of BNP Plasma Level

The plasma BNP concentration was measured with a specific radioimmunoassay for human BNP from 1990 to 1993[9,25,26] and then a specific immunoradiometric assay for human BNP from 1993 to 1999 (Shionoria BNP; Shionogi Inc).[27] There were no significant differences in the BNP values obtained by the radioimmunoassay and immunoradiometric assay methods.[28]

Statistical Analysis

Continuous values are expressed as the mean±SD. Statistical significance was defined as a probability value <0.05. A Cox proportional hazards regression analysis was performed to identify independent predictors of cardiac death by using variables including log BNP, left ventricular ejection fraction, history of heart failure, heart rate, male gender, anterior myocardial infarction, ACE inhibitor or β-blocker use, history of renal dysfunction, age, history of left ventricular hypertrophy, and revascularization. Because the BNP plasma level was not normally distributed, we selected log BNP for analysis. A log BNP cutoff point was selected to define a large patient group with a low risk of cardiac death. A Kaplan-Meier survival curve was used for survival comparisons between patient groups stratified according to this cutoff point.

Results

Follow-Up Periods

The mean follow-up period was 58.6 months (range 1 to 158 months) for all study patients, with mean follow-up periods of 41.3 months (range 1 to 127 months) for the cardiac death group and 61.9 months (range 1 to 158 months) for the non-cardiac-death group.

Prognosis of Patients and Causes of Death

Of the 145 patients, 115 survived and 30 died during the study period. Of the 30 patients who died, 8 (27%) died of sudden death, 15 (50%) had heart failure, and 7 (23%) died of other causes (2 of pneumonia, 2 of lung cancer, 1 of renal cell carcinoma, 1 of liver dysfunction, and 1 of blood dyscrasia).

Comparisons of Clinical Characteristics, Hemodynamic Parameters, and Plasma BNP Levels Between the Cardiac Death Group and the Non-Cardiac-Death Group

The clinical characteristics and hemodynamic parameters of the study patients are shown in Tables 1 and 2. Among all the patients, 72 (50%) had anterior infarction, and 73 (50%) had inferior or posterolateral infarction. Eighty-four (60%) had a history of smoking, 48 (35%) had a history of hypertension, 37 (27%) were obese, 62 (45%) had diabetes mellitus, and 57 (41%) had dyslipidemia (Table 1).

The number of male patients and patients with a history of heart failure was significantly higher in the cardiac death group than in the non-cardiac-death group. There were no significant differences for age, anterior myocardial infarction, coronary risk factors, history of left ventricular hypertrophy, history of renal dysfunction, revascularization, or pharmacotherapy between the cardiac death group and the non-cardiac-death group (Table 1).

TABLE 1. Patients' Characteristics

	Non–Cardiac-Death (n=122)	Cardiac Death (n=23)	P
Age, y	64.7±11.1	66.7±7.9	NS
Male gender	70 (85/122)	91 (21/23)	0.03
Anterior MI	47 (57/122)	65 (15/23)	NS
Smoking	60 (71/119)	65 (13/20)	NS
History of hypertension	37 (44/119)	20 (4/20)	NS
Obesity	28 (33/119)	20 (4/20)	NS
Diabetes mellitus	46 (55/119)	35 (7/20)	NS
History of dyslipidemia	44 (52/119)	25 (5/20)	NS
History of heart failure	4 (5/117)	18 (4/22)	0.015
History of LVH	17 (20/117)	5 (1/22)	NS
History of renal dysfunction	19 (19/102)	33 (6/18)	NS
Revascularization*	53 (62/116)	52 (11/21)	NS
Pharmacotherapy			
ACEI	45 (50/111)	45 (9/20)	NS
Digitalis	3 (3/111)	5 (1/20)	NS
Furosemide	17 (19/111)	25 (5/20)	NS
Spironolactone	3 (3/111)	5 (1/20)	NS
Calcium channel blocker	80 (88/111)	75 (15/20)	NS
Nitrate	59 (65/111)	60 (12/20)	NS
β-Blocker	20 (22/111)	30 (6/20)	NS

Values are percentage (number) of patients or mean±SD. Anterior MI indicates patients with anterior myocardial infarction; LVH, left ventricular hypertrophy.

*Including percutaneous coronary intervention, thrombolytic therapy, and CABG.

Log BNP was significantly higher in the cardiac death group than in the non–cardiac-death group (2.44±0.57 versus 1.91±0.59, $P<0.0001$; Table 2).

Univariate and Multivariate Predictors of Cardiac Death

Table 3 shows the results of univariate and multivariate Cox proportional hazards model analyses for cardiac death. In the univariate analysis, log BNP, left ventricular ejection fraction, history of heart failure, heart rate, and male gender were predictive factors. In the multivariate analysis, log BNP was the only independent predictor of cardiac death.

TABLE 3. Univariate and Multivariate Relations for Prediction of Cardiac Death

	Univariate		Multivariate	
	χ^2	P	χ^2	P
Log BNP	20.06	<0.0001	7.003	0.008
LVEF (%)	7.354	0.007	...	...
History of heart failure	7.304	0.007	...	...
Heart rate, bpm	4.228	0.040	...	...
Male gender	4.096	0.043	...	...
Anterior MI	...	...	...	...
ACEI or β-blocker	...	...	...	...
History of renal dysfunction	...	...	...	...
Age, y	...	...	...	...
History of LVH	...	...	...	...
Revascularization	...	...	...	...

LVEF indicates left ventricular ejection fraction; anterior MI, patients with anterior myocardial infarction; and LVH, left ventricular hypertrophy.

*Including percutaneous coronary intervention, thrombolytic therapy, and CABG.

Kaplan-Meier Survival Analysis

We examined the sensitivity and specificity of various cutoff values of log BNP for predicting survival and created receiver operating characteristic curves. The best value of log BNP with the highest sensitivity and specificity was 2.26, equivalent to a BNP level of up to 180 pg/mL (Figure 1). Figure 2 shows that the survival rates were significantly higher in patients with log BNP <2.26 than in patients with log BNP ≥2.26.

Discussion

During the follow-up period, 23 patients died of cardiac death. The plasma BNP level 3 to 4 weeks after the onset of AMI was significantly higher in the cardiac death group (n=23) than in the non–cardiac-death group (n=122). We examined the sensitivity and specificity of various cutoff values of log BNP for predicting survival. We created

TABLE 2. Hemodynamic Parameters and BNP Levels

	Non–Cardiac-Death (n=122)	Cardiac Death (n=23)	P
Log BNP	1.91±0.59 (81±4 pg/mL)	2.44±0.57 (277±4 pg/mL)	<0.0001
Hemodynamics			
Heart rate, bpm	71±13	80±25	NS
Mean blood pressure, mm Hg	97±15	95±23	NS
SVR, dyne·s·cm^{-5}	1786±52	2209±1039	NS
PVR, dyne·s·cm^{-5}	141±76	223±127	0.0280
LVEDP, mm Hg	11±6	18±5	0.0002
LVEF, %	56±17	44±16	0.0064
CI, L·min^{-1}·m^{-2}	2.3±0.5	2.8±0.6	0.0040

Values are mean±SD. SVR indicates systemic vascular resistance; PVR, pulmonary vascular resistance; LVEDP, left ventricular end-diastolic pressure; LVEF, left ventricular ejection fraction; and CI, cardiac index.

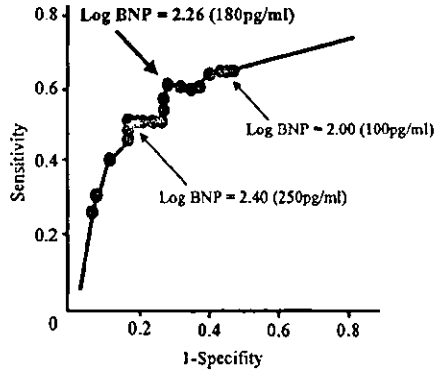

Figure 1. Receiver operating characteristic curves of BNP level for predicting cardiac death. True-positive rates (sensitivity) and false-positive rates (1-specificity) are plotted for various log BNP cutoff values for predicting cardiac death.

receiver operating characteristic curves and concluded that the best cutoff value of log BNP was 2.26, equivalent to a plasma BNP level of 180 pg/mL. The Cox proportional hazards model analysis showed that plasma BNP level was an independent predictor of cardiac death. The survival rate was significantly higher in the patients with log BNP <2.26 (equivalent to a plasma BNP level of up to 180 pg/mL) than in those with log BNP ≥2.26. This plasma BNP level for predicting cardiac events is almost the same as in previous reports.[29–32]

The present study began just after the discovery of BNP, and an antibody for BNP was created by our research group.[9,23] Thus, we were able to follow up patients for a mean period of 58.6 months for all patients, with mean follow-up periods of 41.3 months for the cardiac death group and 61.9 months for the non–cardiac-death group. We demonstrated that the plasma BNP level measured at 3 to 4 weeks after AMI onset was a significant prognostic marker of AMI in this long-term follow-up study.

There have been several reports indicating that the plasma BNP level obtained in the acute phase of AMI can be used as a prognostic marker for patients with AMI[31–37]; however, there are no reports on sampling at 3 to 4 weeks after the onset of AMI. In the present study, we performed BNP sampling at 3 to 4 weeks after AMI onset. Because the changing pattern of the plasma BNP level in patients with AMI is dynamic,[13] the timing

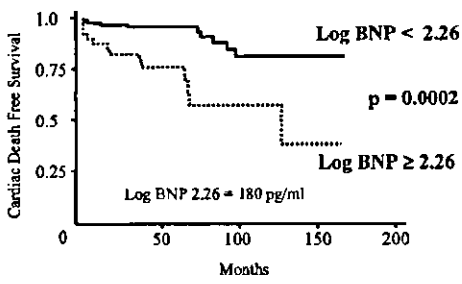

Figure 2. Kaplan-Meier survival curves of cumulative survival rates in patients with AMI divided into 2 groups according to log BNP values. Patients with log BNP ≥2.26 differed significantly from patients with log BNP values below this cutoff point.

of the blood sampling is an important matter. The first peak of plasma BNP was shown ≈20 hours after AMI onset, and the second peak was shown at approximately the fifth day after onset. Plasma BNP levels in the second peak would reflect the degree of ventricular remodeling after AMI.[13] We considered that timing the blood sampling to occur just at the second peak might be ideal to predict prognosis; however, it is quite difficult to obtain the blood sample just at the second peak, because the authentic second peak of plasma BNP varies among patients with AMI. Given this background, a sampling point of 3 to 4 weeks after AMI onset appears better, because plasma BNP levels would be quite stable during this phase, as shown in our previous report.[13] The results of the present study revealed that a sampling time at 3 to 4 weeks after the onset of AMI in addition to the acute phase would provide prognostic insights, as previously speculated.[31,38]

In the present study, the number of patients taking ACE inhibitors (ACEIs) and/or β-blockers appears to be relatively low compared with recent studies[39–43]; it seems that historical background plays a role in accounting for this. There were many patients who participated in the present study around 1995; the rate of calcium channel blocker prescriptions was very high in Japan during that time. We prescribed calcium channel blockers for many patients with AMI, in part because we expected calcium channel blockers to prevent coronary artery spasm, which commonly occurs in Japanese patients.[44] Of course, the use of ACEIs or β-blockers in addition to calcium channel blockers is increasing even now in Japan. It has been reported that ACEIs are useful in the treatment of heart failure after AMI[39–42]; thus, it would be highly recommended that an ACEI be prescribed, or that the dose of the ACEI be increased, if the plasma BNP level is elevated 3 to 4 weeks after the onset of AMI. In addition, an aldosterone antagonist would be useful in the treatment of AMI.[45] In the present study, baseline medications, such as ACEIs or β-blockers, were not related to plasma BNP levels (data not shown) or the prognosis of the study patients (Table 3).

In our previous report, we stated that the biphasic pattern of the plasma BNP level indicated poor ventricular function after AMI, whereas the monophasic pattern did not.[13] Plasma BNP levels at 3 to 4 weeks after AMI onset were higher in the biphasic pattern than in the monophasic pattern. This observation and the present data suggest that the biphasic pattern would indicate a poor prognosis after AMI.

In the present long-term follow-up study, we found that plasma levels of BNP measured at 3 to 4 weeks after AMI were a prognostic marker statistically; however, the sample size was limited. Thus, it might be necessary to perform analysis on a larger scale in another series of studies. It is also necessary to examine how BNP levels at 3 to 4 weeks after the onset of AMI affect the subsequent treatment, including medical therapies and implantation of an internal defibrillator.

In conclusion, the plasma BNP level measured 3 to 4 weeks after the onset of AMI is a significant prognostic marker of AMI, as determined by this long-term follow-up study.

Acknowledgments

This study was supported in part by grants-in-aid for the Ministry of Education, Culture, Sports, Science, and Technology, Tokyo [B

(2)-15390248 and B (2)-15390249], the Ministry of Health, Labor and Welfare, Tokyo (14C-4 and 14A-1), and the Smoking Research Foundation, Tokyo.

References

1. Laragh JH. Atrial natriuretic hormone, the renin-aldosterone axis, and blood pressure–electrolyte homeostasis. *N Engl J Med.* 1985;313: 1330–1340.
2. Needleman P, Greenwald JE. Atriopeptin: a cardiac hormone intimately involved in fluid, electrolyte and blood-pressure homeostasis. *N Engl J Med.* 1986;314:828–834.
3. Floras JS. Sympathoinhibitory effects of atrial natriuretic factor in normal humans. *Circulation.* 1990;81:1860–1873.
4. Burnett JC Jr, Kao PC, Hu DC, et al. Atrial natriuretic peptide elevation in congestive heart failure in the human. *Science.* 1986;231:1145–1147.
5. Raine AEG, Erne P, Burgisser E, et al. Atrial natriuretic peptide and atrial pressure in patients with congestive heart failure. *N Engl J Med.* 1986; 315:533–537.
6. Saito Y, Nakao K, Nishimura K, et al. Clinical application of atrial natriuretic polypeptide in patients with congestive heart failure: beneficial effects on left ventricular function. *Circulation.* 1987;76:115–124.
7. Yoshimura M, Yasue H, Morita E, et al. Hemodynamic, renal, and hormonal responses to brain natriuretic peptide infusion in patients with congestive heart failure. *Circulation.* 1991;84:1581–1588.
8. Yasue H, Obata K, Okumura K, et al. Increased secretion of atrial natriuretic polypeptide (ANP) from the left ventricle in the patients with dilated cardiomyopathy. *J Clin Invest.* 1989;83:46–51.
9. Mukoyama M, Nakao K, Hosoda K, et al. Brain natriuretic peptide as a novel cardiac hormone in humans: evidence for an exquisite dual natriuretic peptide system, atrial natriuretic peptide and brain natriuretic peptide. *J Clin Invest.* 1991;91:1402–1412.
10. Yasue H, Yoshimura M, Sumida H, et al. Localization and mechanism of secretion of B-type natriuretic peptide in comparison with those of A-type natriuretic peptide in normal subjects and patients with heart failure. *Circulation.* 1994;90:195–203.
11. Yoshimura M, Yasue H, Okumura K, et al. Different secretion patterns of atrial natriuretic peptide and brain natriuretic peptide in patients with congestive heart failure. *Circulation.* 1993;87:464–469.
12. Nakagawa O, Ogawa Y, Itoh H, et al. Rapid transcriptional activation and early MRNA turnover of brain natriuretic peptide in cardiocyte hypertrophy. *J Clin Invest.* 1995;96:1280–1287.
13. Morita E, Yasue H, Yoshimura M, et al. Increased plasma levels of brain natriuretic peptide in patients with acute myocardial infarction. *Circulation.* 1993;88:82–91.
14. de Lemos JA, Morrow DA, Bentley JH, et al. The prognostic value of B-type natriuretic peptide in patients with acute coronary syndromes. *N Engl J Med.* 2001;345:1014–1021.
15. Sumida H, Yasue H, Yoshimura M, et al. Comparison of secretion pattern between A-type and B-type natriuretic peptides in patients with old myocardial infarction. *J Am Coll Cardiol.* 1995;25:1105–1110.
16. Mukoyama M, Nakao K, Obata K, et al. Augmented secretion of brain natriuretic peptide in acute myocardial infarction. *Biochem Biophys Res Commun.* 1991;180:431–436.
17. Kojima M, Minamoto N, Kangawa K, et al. Cloning and sequence analysis of cDNA encoding a precursor for rat brain natriuretic peptide. *Biochem Biophys Res Commun.* 1989;159:1420–1426.
18. Kushner I. The phenomenon of the acute phase response. *Ann N Y Acad Sci.* 1982;389:39–48.
19. Harada E, Nakagawa O, Yoshimura M, et al. Effect of interleukin-1 beta on cardiac hypertrophy and production of natriuretic peptides in rat cardiocyte culture. *J Mol Cell Cardiol.* 1999;31:1997–2006.
20. Shubeita HE, McDonough PM, Harris AN, et al. Endothelin induction of inositol phospholipid hydrolysis, sarcomere assembly, and cardiac gene expression in ventricular myocytes: a paracrine mechanism for myocardial cell hypertrophy. *J Biol Chem.* 1990;265:20555–20562.
21. Baker KM, Aceto JF. Angiotensin II stimulation of protein synthesis and cell growth in chick heart cells. *Am J Physiol Heart Circ Physiol.* 1990;259:610–618.
22. Conti E, Andreotti F, Sciahbasi A, et al. Markedly reduced insulin-like growth factor-1 in the acute phase of myocardial infarction. *J Am Coll Cardiol.* 2001;38:26–32.
23. Saito Y, Nakao K, Itoh H, et al. Brain natriuretic peptide is a novel cardiac hormone. *Biochem Biophys Res Commun.* 1989;158:360–368.
24. Sudoh T, Kangawa K, Minamino N, et al. A new natriuretic peptide in porcine brain. *Nature.* 1988;332:78–81.
25. Mukoyama M, Nakao K, Saito Y, et al. Human brain natriuretic peptide, a novel cardiac hormone. *Lancet.* 1990;335:801–802.
26. Mukoyama M, Nakao K, Saito Y, et al. Increased human brain natriuretic peptide in congestive heart failure. *N Engl J Med.* 1990;323:757–758.
27. Kono M, Yamaguchi A, Tsuji T, et al. An immunoradiometric assay for brain natriuretic peptide in human plasma. *Kaku Igaku.* 1993;13:2–7.
28. Yasue H, Yoshimura M, Jougasaki M, et al. Plasma levels of brain natriuretic peptide in normal subjects and patients with chronic congestive heart failure: measurement by immunoradiometric assay (IRMA). *Horm Clin.* 1993;41:397–403.
29. Anand IS, Fisher LD, Chiang YT, et al, for the Val-HeFT Investigators. Changes in brain natriuretic peptide and norepinephrine over time and mortality and morbidity in the Valsartan Heart Failure Trial (Val-HeFT). *Circulation.* 2003;107:1278–1283.
30. Berger R, Huelsman M, Strecker K, et al. B-type natriuretic peptide predicts sudden death in patients with chronic heart failure. *Circulation.* 2002;105:2392–2397.
31. Omland T, Aakvaag A, Bonarjee VV, et al. Plasma brain natriuretic peptide as an indicator of left ventricular systolic function and long-term survival after acute myocardial infarction: comparison with plasma atrial natriuretic peptide and N-terminal proatrial natriuretic peptide. *Circulation.* 1996;93:1963–1969.
32. Richards AM, Nicholls MG, Espiner EA, et al. B-type natriuretic peptides and ejection fraction for prognosis after myocardial infarction. *Circulation.* 2003;107:2786–2792.
33. Arakawa N, Nakamura M, Aoki H, et al. Plasma brain natriuretic peptide concentrations predict survival after acute myocardial infarction. *J Am Coll Cardiol.* 1996;27:1656–1661.
34. Darbar D, Davidson NC, Gillespie N, et al. Diagnostic value of B-type natriuretic peptide concentrations in patients with acute myocardial infarction. *Am J Cardiol.* 1996;78:284–287.
35. Palmer BR, Pilbrow AP, Yandle TG, et al. Angiotensin-converting enzyme gene polymorphism interacts with left ventricular ejection fraction and brain natriuretic peptide levels to predict mortality after myocardial infarction. *J Am Coll Cardiol.* 2003;41:729–736.
36. James SK, Lindahl B, Siegbahn A, et al. N-terminal pro-brain natriuretic peptide and other risk markers for the separate prediction of mortality and subsequent myocardial infarction in patients with unstable coronary artery disease. *Circulation.* 2003;108:275–281.
37. Omland T, Persson A, Ng L, et al. N-terminal pro-B-type natriuretic peptide and long-term mortality in acute coronary syndromes. *Circulation.* 2002;106:2913–2918.
38. Bonow RO. New insights into the cardiac natriuretic peptides. *Circulation.* 1996;93:1946–1950.
39. Pfeffer MA, Braunwald E, Moye LA, et al. Effect of captopril on mortality and morbidity in patients with left ventricular dysfunction after myocardial infarction: results of the Survival And Ventricular Enlargement trial: the SAVE Investigators. *N Engl J Med.* 1992;327: 669–677.
40. Køber L, Torp-Pedersen C, Carlsen JE, et al. A clinical trial of the angiotensin-converting-enzyme inhibitor trandolapril in patients with left ventricular dysfunction after myocardial infarction: Trandolapril Cardiac Evaluation (TRACE) Study Group. *N Engl J Med.* 1995;333:1670–1676.
41. Hall AS, Murray GD, Ball SG. Follow-up study of patients randomly allocated ramipril or placebo for heart failure after acute myocardial infarction: AIRE Extension (AIREX) Study: Acute Infarction Ramipril Efficacy. *Lancet.* 1997;349:1493–1497.
42. Yusuf S, Sleight P, Pogue J, et al. Effects of an angiotensin-converting–enzyme inhibitor, ramipril, on cardiovascular events in high-risk patients: the Heart Outcomes Prevention Evaluation Study Investigators. *N Engl J Med.* 2000;342:145–153.
43. ISIS-1 (First International Study of Infarct Survival) Collaborative Group. Randomised trial of intravenous atenolol among 16027 cases of suspected acute myocardial infarction: ISIS-1. *Lancet.* 1986;2:57–66.
44. Yasue H, Kugiyama K. Coronary spasm: clinical features and pathogenesis. *J Intern Med.* 1997;36:760–765.
45. Pitt B, Remme W, Zannad F, et al. Eplerenone, a selective aldosterone blocker, in patients with left ventricular dysfunction after myocardial infarction. *N Engl J Med.* 2003;348:1309–1321.

Overexpression of Brain Natriuretic Peptide Facilitates Neutrophil Infiltration and Cardiac Matrix Metalloproteinase-9 Expression After Acute Myocardial Infarction

Rika Kawakami, MD; Yoshihiko Saito, MD, PhD; Ichiro Kishimoto, MD, PhD; Masaki Harada, MD, PhD; Koichiro Kuwahara, MD, PhD; Nobuki Takahashi, MD; Yasuaki Nakagawa, MD; Michio Nakanishi, MD; Keiji Tanimoto, MD; Satoru Usami, MD; Shinji Yasuno, MD; Hideyuki Kinoshita, MD; Hideki Chusho, MD, PhD; Naohisa Tamura, MD, PhD; Yoshihiro Ogawa, MD, PhD; Kazuwa Nakao, MD, PhD

Background—Recent clinical trials have shown that systemic infusion of nesiritide, a recombinant human brain natriuretic peptide (BNP), improves hemodynamic parameters in acutely decompensated hearts. This suggests that BNP exerts a direct cardioprotective effect and might thus be a useful therapeutic agent with which to treat acute myocardial infarction (MI). In the present study, we used BNP-transgenic (BNP-Tg) mice with elevated plasma BNP to determine whether and how BNP contributes to left ventricular remodeling and healing after MI.

Methods and Results—We examined the accumulation of neutrophils and the expression and activation of matrix metalloproteinase (MMP)-9 in the ventricles of male BNP-Tg mice and their nontransgenic (non-Tg) littermates during the early phase after acute MI. The numbers of neutrophils infiltrating the infarcted area were significantly increased in BNP-Tg mice 3 days after MI. In addition, both the gene expression and zymographic activity of MMP-9, but not MMP-2, were significantly higher in BNP-Tg than non-Tg mice. Double immunostaining revealed that neutrophils are the main source of the MMP-9, although doxycycline, an MMP inhibitor, had no effect on neutrophil infiltration of the infarcted area in BNP-Tg mice.

Conclusions—These results demonstrate that elevated plasma BNP facilitates neutrophil infiltration of the infarcted area after MI and increases the activity of the MMP-9 they produce. This suggests that BNP plays a key role in the processes of extracellular matrix remodeling and wound-healing during the early phase after acute MI. (***Circulation***. **2004;110: 3306-3312.)**

Key Words: metalloproteinases ■ myocardial infarction ■ natriuretic peptides ■ remodeling ■ neutrophils

By secreting both atrial and brain natriuretic peptides (ANP and BNP, respectively), which act via natriuretic peptide receptor A (NPRA) to induce natriuresis, diuresis, and vasodilation and to inhibit the renin-angiotensin-aldosterone and sympathetic nervous systems, the heart serves as an important endocrine organ involved in the regulation of blood pressure and fluid-electrolyte balance.[1,2] ANP is synthesized and secreted primarily from the atria in adult mammals, whereas BNP is secreted primarily from the ventricle.[3] Synthesis and secretion of both ANP and BNP are markedly increased in patients with congestive heart failure.[4] Plasma BNP levels are also strongly increased during the early phase of acute myocardial infarction (MI), although plasma ANP levels are increased only slightly.[5] Such sustained increases in plasma BNP are correlated with enlargement of the left ventricle (LV), decreased ventricular contractility, and increased ventricular stiffness,[6,7] which suggests that BNP might play a significant role in ventricular remodeling. In fact, using BNP-deficient mice, we previously showed that endogenous BNP is a local regulator of ventricular fibrosis.[8]

Intravenous infusion of nesiritide, a recombinant human BNP, was recently reported to have beneficial hemodynamic effects in patients with decompensated congestive heart failure.[9,10] In addition to alleviating cardiac preload and afterloads, BNP might exert a direct cardioprotective effect[11,12] that could prevent LV remodeling after MI. The

Received January 4, 2004; de novo received June 8, 2004; accepted July 7, 2004.

From the Department of Medicine and Clinical Science, Kyoto University Graduate School of Medicine, Kyoto, Japan. Dr Saito is now at the First Department of Internal Medicine, Nara Medical University, Nara, Japan.

The online-only Data Supplement, which contains an additional figure, can be found with this article at http://www.circulationaha.org.

Correspondence to Ichiro Kishimoto, National Cardiovascular Center, 5-7-1 Fujishiro-dai, Suita, Osaka, 565-8565, Japan. E-mail kishimot@ri.ncvc.go.jp

Circulation **is available at http://www.circulationaha.org** **DOI: 10.1161/01.CIR.0000147829.78357.C5**

effects of continuously high levels of BNP on the infarcted myocardium are unknown, however. We therefore used BNP-transgenic (BNP-Tg) mice to investigate the effects of sustained increases in plasma BNP on cardiac repair pathways and remodeling after MI. These mice overexpress the BNP in their livers and show a >100-fold increase in plasma BNP levels throughout their lives.[13,14] In the present study, we focused on leukocyte infiltration, the genetic regulation of myocardial collagen synthesis including transforming growth factor (TGF)-β, and the activity of matrix metalloproteinase (MMP)-9, an important regulatory enzyme involved in extracellular matrix (ECM) degradation and cell migration during cardiac wound healing,[15,16] in infarcted BNP-Tg hearts.

Methods

Experimental Animals

BNP-Tg mice were developed as previously described[13] by use of the liver-specific human serum amyloid P component promoter. These mice show plasma BNP concentrations that are at least 2 orders of magnitude higher than those of their wild-type littermates, C57BL/6J nontransgenic (non-Tg) mice. Acute MI was induced in male BNP-Tg (n=51) and non-Tg (n=43) mice (age, 8 to 12 weeks; weight, 25 to 30 g) by ligation of the left coronary artery.[17,18] The same procedure without coronary artery ligation served as the sham operation. The experimental animals were monitored for 7 days after MI had been induced.

Echocardiography

Echocardiography was performed under light anesthesia with a mixture of ketamine (80 mg/kg) and xylazine (4 mg/kg) and spontaneous respiration.[19]

Hemodynamic and Infarct Size Measurements

After 3 days, a 2F Millar Micro-Tip catheter transducer (Millar Instruments) was inserted into the right carotid artery and then advanced into the LV for recording of LV systolic pressure, LV end-diastolic pressure, and LV maximum and minimum rates of pressure development (dP/dt). The ventricles were excised after evaluation of hemodynamic parameters. Infarct size was expressed as the ratio of the infarct to total LV mass as previously described.[17]

Immunohistochemistry and Quantitative Analysis of Histology

In a subset of animals (6 BNP-Tg and 6 non-Tg), the LV was cut into 3 transverse sections (apex, middle ring, and base) 3 days after MI. Immunostaining was then performed on frozen tissue specimens (6 μm) with rat anti-mouse 7/4 antibody (Serotec), which recognizes a polymorphic 40-kDa antigen expressed by neutrophils, and goat anti-mouse MMP-9 antibody (Santa Cruz Biotechnology). For each section, neutrophil 7/4-positive cells were counted in the infarcted area in at least 8 to 10 randomly selected high-power fields by use of a computer program (KS400 Version 3.00; Carl Zeiss).

Myeloperoxidase Activity Assay

Myeloperoxidase (MPO) activity was measured spectrophotometrically at 460 nm in 50 mmol/L phosphate buffer (pH 6.0) containing 0.167 mg/mL *o*-dianisidine hydrochloride (Sigma) and 0.0005% hydrogen peroxide as described previously.[20] One unit of MPO was defined as the quantity of enzyme needed to hydrolyze peroxide at a rate of 1 mmol/min at 25°C.

Northern Blot Analysis

Northern blots were made using 20 μg of total RNA isolated from frozen LV tissue by use of a technique described in detail elsewhere.[8] The probes for collagen I, collagen III, TGF-β_1, TGF-β_3, fibronectin and BNP were already available to us.[8] The other cDNA probes were prepared using reverse transcription–polymerase chain reaction with primers based on the published sequences.

Zymographic Measurement of Gelatinase Activity

MMP activity in 30 μg of myocardial extract was measured by gelatin zymography as previously described.[21,22] The gelatinolytic zones were quantified by use of NIH 1.62 image analysis software.[22]

Type IV Collagenase Activity Assay

The activity of type IV collagenases (MMP-2 and MMP-9) was assessed by use of a commercially available kit (Yagai Research Center) according to the manufacturer's instructions.[23]

Treatment With Doxycycline

In the doxycycline study, mice receiving 60 mg/kg doxycycline per day by gavage were compared with an untreated control group. Administration of doxycycline was started 3 days before induction of experimental MI and continued for 7 days after MI.

Data Analysis

All results are reported as mean±SEM. Two-way ANOVA followed by Tukey-Kramer tests was used to evaluate the effects of MI and genotype. The mortality data (deaths during the 7-day protocol, including causes of death) were analyzed by use of the χ^2 test. Values of $P<0.05$ were considered significant.

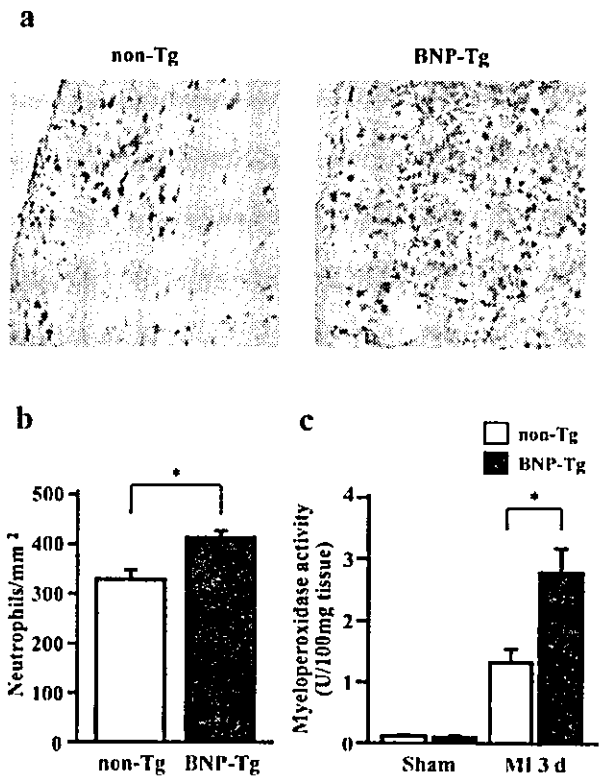

Figure 1. Accumulation of neutrophils in hearts of infarcted mice. a, Representative micrograph showing stained neutrophils within infarcted region (magnification ×200). b, Numbers of neutrophils per mm² within infarcted area 3 days after MI (n=6 for each). c, Cardiac MPO activity expressed as units/100 mg tissue wet wt in sham-operated and infarcted mice 3 days after MI (n=8 for each). Values are mean±SEM; *$P<0.01$ vs non-Tg mice with MI.